Water Research 219 (2022) 118565

Contents lists available at ScienceDirect

Water Research

journal homepage: www.elsevier.com/locate/watres

The *in-situ* release of algal bloom populations and the role of prokaryotic communities in their establishment and growth

Xiao Ma [a,b], Kevin B. Johnson [c], Bowei Gu [a,d], Hao Zhang [a,b], Gang Li [a,b], Xiaoping Huang [a,b], Xiaomin Xia [a,b,*]

[a] Key Laboratory of Tropical Marine Bio-Resources and Ecology, South China Sea Institute of Oceanology, Chinese Academy of Sciences, Guangzhou, China
[b] Southern Marine Science and Engineering Guangdong Laboratory (Guangzhou), China
[c] Department of Ocean Engineering and Marine Sciences, Florida Institute of Technology, Melbourne, FL, United States
[d] University of Chinese Academy of Sciences, Beijing, China

ARTICLE INFO

Keywords:
Algal bloom population dynamics
Diatom
Dinoflagellate
Prokaryotic community composition and function
Planctomycetaceae

ABSTRACT

Harmful algal blooms (HABs) may quickly travel and inoculate new water bodies via currents and runoff in estuaries. The role of *in-situ* prokaryotic communities in the re-establishment and growth of inoculated algal blooms remains unknown. A novel on-board incubation experiment was employed to simulate the sudden surge of algal blooms to new estuarine waters and reveal possible outcomes. A dinoflagellate (*Amphidinium carterae*) and a diatom species (*Thalassiosira weissflogii*) which had bloomed in the Pearl River Estuary (PRE) area were cultured to bloom densities and reintroduced back into PRE natural seawaters. The diatom showed better adaptation ability to the new environment and increased significantly after the incubation. Simultaneously, particle-attached (PA) prokaryotic community structure was strongly influenced by adding of the diatom, with some opportunistic prokaryotes significantly enhanced in the diatom treatment. Whereas the dinoflagellate population did not increase following incubation, and their PA prokaryotic community showed no significant differences relative to the control. Metagenomic analyzes revealed that labile carbohydrates and organic nitrogen produced by the diatom contributed to the surge of certain PA prokaryotes. Genomic properties of a bacteria strain, which is affiliated with genus GMD16E07 (Planctomycetaceae) and comprised up to 50% of PA prokaryotes in the diatom treatment, was described here for the first time. Notably, the association of Planctomycetaceae and *T. weissflogii* likely represents symbiotic mutualism, with the diatom providing organic matter for Planctomycetaceae and the bacteria supplying vitamins and detoxifying nitriles and hydrogen peroxides in exchange. Therefore, the close association between Planctomycetaceae and *T. weissflogii* promoted the growth of both populations, and eventually facilitated the diatom bloom establishment.

1. Introduction

Algal blooms are an increasing problem in estuaries around the world due to increasing human activity and climate change (Berry et al., 2015; Cao et al., 2017; Phlips et al., 2015). Algae and prokaryotes commonly interact in aquatic systems, and algal blooms may alter the prokaryotic community and its ecological functions (Camarena-Gómez et al., 2021; Cui et al., 2020; Zhou et al., 2020). Many studies have demonstrated bloom stage-specific host-specificity in algal-associated prokaryotic communities for different algal species. Thus, microbial behavior and succession patterns in phycosphere microenvironments may contribute to algal bloom formation and longevity (Alavi et al.,

Abbreviations: HABs, harmful algal blooms; PRE, Pearl River Estuary; AC, *Amphidinium carterae*; TW, *Thalassiosira weissflogii*; PA, Particle-attached; FL, Free-living; PC, Polycarbonate; DOC, Dissolved Organic Carbon; OTUs, Operational Taxonomic Units; "E_OTU", OTUs from incubation experiment dataset; "_un", unidentified; ACE, Abundance-based Coverage Estimator; ORFs, Open Reading Frames; TPM, Transcripts Per Million; nMDS, Nonmetric Multidimensional Scaling; STAMP, Statistical Analysis of Metagenomic Profiles; CAZymes, Carbohydrate-Active Enzymes; AAs, Auxiliary Activities; CBMs, Carbohydrate-Binding Modules; CEs, Carbohydrate Esterases; GHs, Glycoside Hydrolases; GTs, Glycosyl Transferases; ABC-transporters, ATP-binding cassette transporters; PTS, Phosphotransferase System; EPS, extracellular polymeric substance.

* Corresponding author at: Key Laboratory of Tropical Marine Bio-Resources and Ecology, South China Sea Institute of Oceanology, Chinese Academy of Sciences, Guangzhou, China.
E-mail address: xiaxiaomin@scsio.ac.cn (X. Xia).

https://doi.org/10.1016/j.watres.2022.118565
Received 28 December 2021; Received in revised form 3 May 2022; Accepted 5 May 2022
Available online 12 May 2022

2001; Amin et al., 2012; Choi et al., 2018; Green et al., 2004; Zhang et al., 2018). In addition, modern "omics" studies have provided evidence of a linkage between changes in prokaryotic community functional genes and shifting organic matter cycles throughout different bloom stages (Brussaard et al., 2017; Durham et al., 2015; Zhou et al., 2020). Understanding the interactions between algae and associated prokaryotic communities will help clarify the mechanisms that mediate algal bloom dynamics (Choi et al., 2018; Liu et al., 2019; Ramanan et al., 2016; Sun et al., 2018). The study of algal-bacterial relationship is gaining attention, often focusing on bloom management and prevention (Coyne et al., 2022; Yong et al., 2021). However, prokaryotic functional profiles and their biogeochemical potential in algal bloom processes remain poorly understood. This study aims to examine algal-bacterial association under *in-situ* bloom re-establishment conditions in estuarine waters.

Planktonic algal blooms may be transported over long distances via currents and runoff (Paerl et al., 2018). For example, a toxic dinoflagellate bloomed on the coast of North Carolina after the seed population was carried by the Gulf Stream over 800 km from the source bloom site (Tester et al., 1991); a massive phytoplankton bloom initiated in the Great Barrier Reef lagoon spread 150 km in nine days via a river plume (Brodie et al., 2010). Algal bloom expansion could rapidly change local water column physico-chemical factors, such as turbidity, dissolved organic carbon, nutrients and dissolved oxygen. It may also induce a sudden shift of prokaryotic community structure and function. Attempts have been made to study prokaryotic community succession during algal blooms in fixed stations (Berry et al., 2017; Cui et al., 2020; Liu et al., 2019; Zhou et al., 2020, 2018). Some *in-situ* algal bloom monitoring has confirmed prokaryotic community succession during bloom events, raising the possibility that specific prokaryotic populations may occupy transitory ecological niches associated with particular bloom stages (Choi et al., 2018; Wemheuer et al., 2014; Zhou et al., 2020). However, few studies have examined the impacts of algal bloom phase on the local prokaryotic community. This is because it is difficult to precisely predict algal bloom onset and progression in a natural open water system (Allen et al., 2008; Stumpf et al., 2009). In this study, a novel method was employed to simulate the inoculation of estuarine algal blooms to new waters. Comparative incubation experiments were carried out at four stations in the Pearl River Estuary (PRE) to unveil the effects of prokaryotic community composition and function changes on the algal bloom re-establishment and growth.

The PRE, also known as the Great Bay Area is one of the most urbanized and populated estuaries in the world. Like other estuarine systems, harmful algal blooms (HABs) are a recurring problem in the PRE, with 337 HABs, mostly dinoflagellates and diatoms, reported from 1980 to 2016 (Li et al., 2019). The PRE has an annual average discharge of 10,000 cubic meters per second, and is subject to monsoon seasonality, with a strong northeasterly season in winter, and a weak southwesterly season in summer (Pan et al., 2020). The complex energetic circulation and high river discharge at ebb tide can lead to river plumes, in which buoyant masses of brackish water travel on top of dense ocean water, with a persistent surface lens traveling considerable distances (Devlin and Pan, 2018). Thus, algal blooms formed at PRE are likely to be transported to the adjacent outer coastal region within few hours or days. To test what happens to the prokaryotic community when the seeds of a bloom are delivered to a coastal region, one dinoflagellate (*Amphidinium carterae*) and one diatom species (*Thalassiosira weissflogii*), which had bloomed in the PRE area, were selected and cultured to bloom densities in the lab (Li et al., 2013; Lu et al., 2014). They were then introduced and incubated in natural seawater at different stations to simulate the quick invasion of algal blooms to different locations in an estuarine system. This study aimed to 1) test whether different algal blooms would re-establish when they are introduced to new water bodies; 2) evaluate the potential effects of the transplanted algal blooms on prokaryotic community abundance, composition and function; 3) identify the key prokaryotic species that respond to the algal bloom and unveil the interspecies interaction mechanisms.

2. Materials and methods

2.1. Study sites and sample collections

This study was carried out from August 18–25th 2020, during a cruise in the PRE. Surface seawater (0.5 m depth) was collected from sampling stations indicated in Fig. 1A, using a 5 L polymethyl methacrylate water sampler. The 3 μm pore-size was used for distinguishing free-living (FL) from particle-attached (PA) prokaryotes (Liu et al., 2019; Schmidt et al., 2016; Teeling et al., 2012). Water collected from each station was prefiltered with 200 μm mesh to exclude mesozooplankton, and then filtered through 3 μm (collecting PA prokaryotes) and 0.2 μm (collecting FL prokaryotes) polycarbonate (PC) membranes (Millipore) successively. Membranes were kept at −80 °C until DNA extraction. Samples ($n = 3$) for flow cytometry analysis (1.8 mL) were also collected at each station. They were preserved with 0.5% buffered paraformaldehyde (v/v, final concentration), and stored in a −80 °C freezer until analysis. Water temperature, salinity and pH were measured using a YSI multiprobe sensor, which was calibrated before each sampling. Water samples ($n = 3$) for inorganic nutrients and dissolved organic carbon (DOC) analysis were prefiltered with GF/F membranes and collected in 50 mL sterile centrifuge tubes at each station and treatment. Nutrient concentrations including inorganic forms of nitrate, nitrite, ammonia, phosphate and silicate were determined using a segmented continuous flow nutrient autoanalyzer (SEAL AA3) following the manufacture's methods. DOC was measured using total organic carbon analyzers (Shimadzu TOC-L series) utilizing the 680 °C combustion catalytic oxidation method.

2.2. Incubation experiments setup and sample collections

Incubation experiments were conducted at selected medium salinity stations (S10 and S17; with salinities of 23 and 25, respectively), and high salinity stations (S15 and S19; with salinities of 29 and 31, respectively) (Fig. 1). For incubation experiments, surface seawater was prefiltered with 200 μm mesh to exclude larger zooplankton. Three treatments were setup at each station. They were seawater control, dinoflagellate treatment (inoculated with *A. carterae*) and diatom treatment (inoculated with *T. weissflogii*). At the beginning of the incubation experiments, the densities of inoculated *A. carterae* ranged from 1×10^3 to 1×10^4 cells mL^{-1}, and the densities of *T. weissflogii* varied from 1×10^4 to 1×10^5 cells mL^{-1} (Fig. 2A). These inoculum concentrations were selected based on natural bloom densities recorded in the previous studies, where the highest diatom bloom density was an order-of-magnitude higher than the dinoflagellate bloom (Gárate-Lizárraga et al., 2019; Seebah et al., 2014). The relative abundances of background phytoplankton were low in all treatments (Table S2, Fig. S2). Experimental densities were analogous to natural blooms where bloom species dominated phytoplankton communities. The cell densities of inoculated *T. weissflogii* were 1.15 to 5.39 times higher than that of *A. carterae* at the onset of experiments and we acknowledge a possible bias of different initial inoculum total cell densities when comparing dinoflagellate and diatom results. Both *A. carterae* and *T. weissflogii* were precultured in the lab using 1 L PC bottles using Guillard's (F/2) medium at 25 °C with a 14:10 light: dark cycle (Hoff and Snell, 2007). Both algal cultures were in the exponential growth phase and acclimated to 29 °C before experiments. At each station, cultures were washed gently through a 5 μm mesh PC membrane (Millipore) with 0.2 μm prefiltered *in situ* seawater to remove the growth medium (Fig. 1B). Washed algal cultures were then resuspended gently using a Pasteur pipet with 200 μm prefiltered *in situ* seawater (Fig. 1B). Both *A. carterae* and *T. weissflogii* were precultured at two salinities, 25 and 30. At the stations with salinity near 25 (S10 and S17), algae precultured at a salinity of 25 were added. At the stations with salinity near 30 (S15 and S19), algae precultured at a

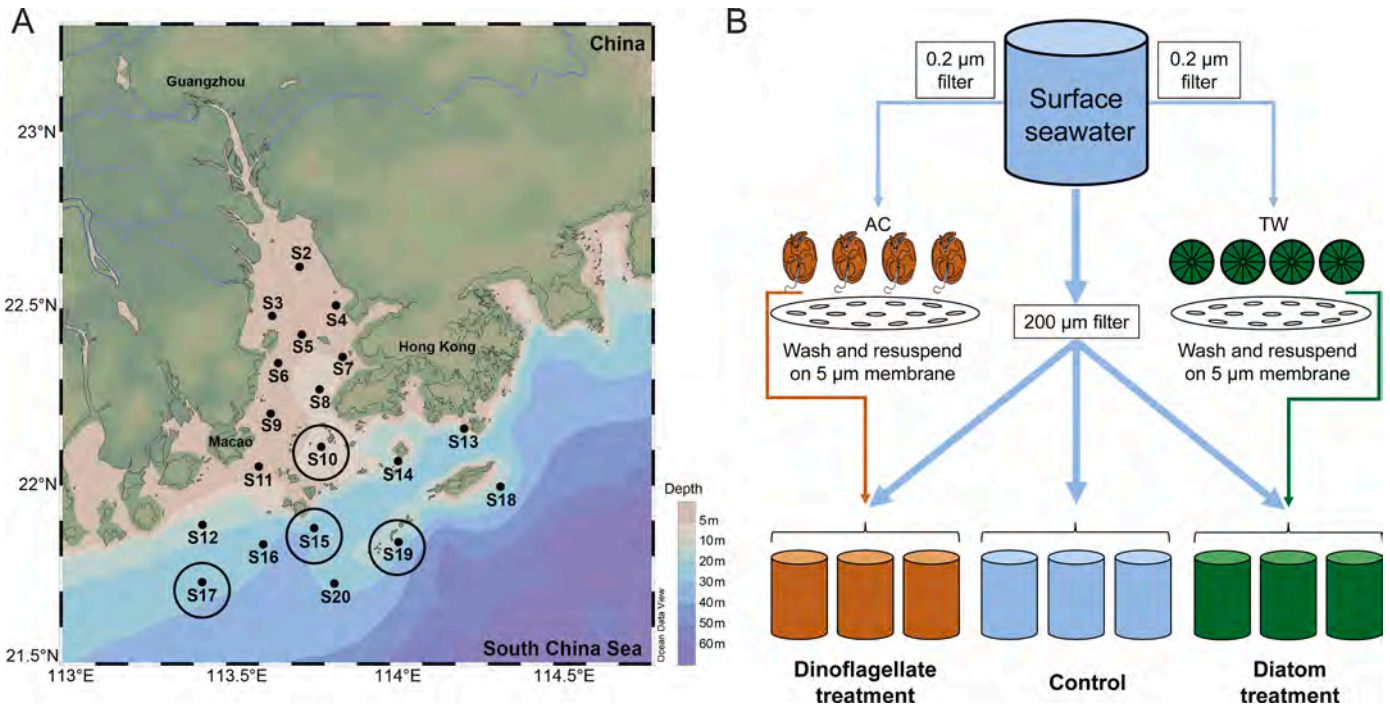

Fig. 1. (A) PRE sampling stations. Black circles indicate the stations where incubation experiments were conducted. The map was generated by Ocean Data View (version 5.5.1). (B) Diagram of the incubation experiment setup. At each incubation station, surface seawater was prefiltered with 200 μm mesh and divided into three treatments, which were control, dinoflagellate treatment and diatom treatment. For the algal treatments, both the dinoflagellate (AC) and the diatom (TW) were washed and resuspended on 5 μm membrane with 0.2 μm prefiltered seawater to remove the growth medium, and then inoculated to 200 μm prefiltered *in situ* seawater.

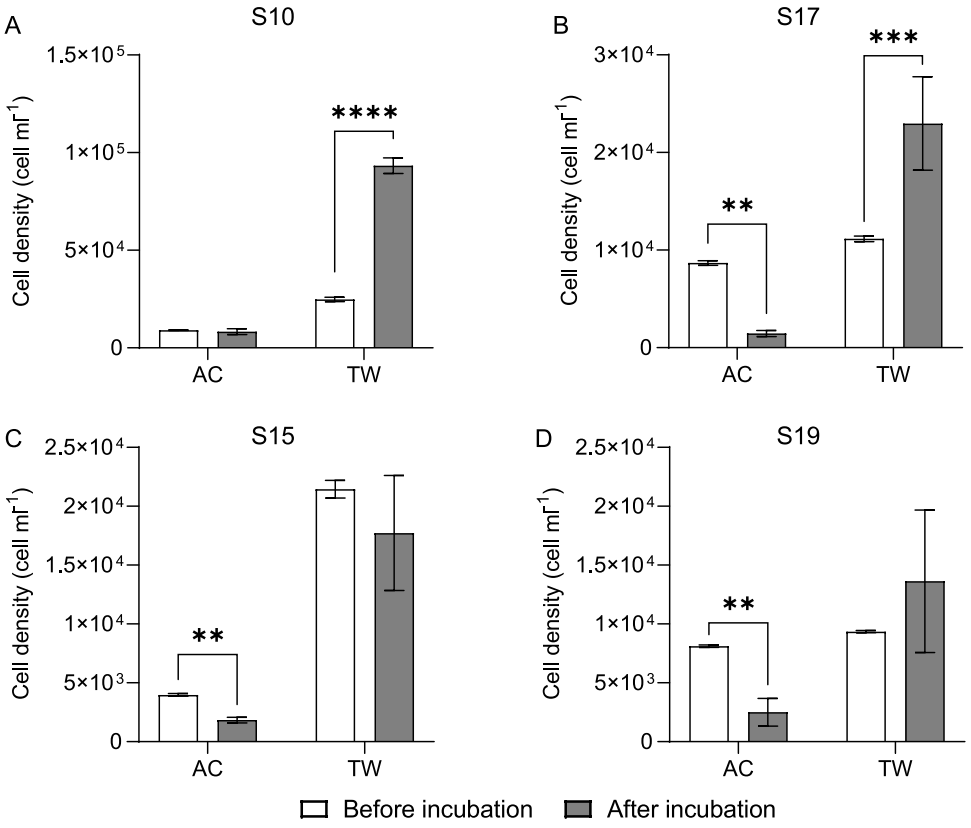

Fig. 2. The cell densities (Mean ± SD) of the inoculated dinoflagellate (AC) and diatom (TW) before versus after incubation at (A) S10, (B) S17, (C) S15 and (D) S19. Different significance levels were determined via Two-way ANOVA and Fisher's LSD test ($\alpha = 0.05$), where ** indicates $p < 0.01$, *** indicates $p < 0.001$, **** indicates $p < 0.0001$.

salinity of 30 were added. Incubation experiments were performed in 1 L PC bottles. These bottles were soaked in 10% HCl-Nanopure water for 24 h and rinsed 3 times with ultra-pure water before the experiments. Three replicates ($n = 3$) were run for each of the three treatments. During incubation, PC bottles were submerged in a 1.5 m × 1 m × 0.5 m deckside water bath with flow-through ambient surface water, maintaining the same temperature as the oceanographic station. *In situ* water column light conditions were simulated with neutral density screening. After 48 h of incubation, 500 mL of water from each bottle was filtered through 3 and 0.2 μm PC membranes successively. Membranes were kept at −80 °C until DNA extraction. Water samples ($n = 3$) for nutrient analyzes were prefiltered through GF/F membranes and collected in 50 mL sterile centrifuge tubes after incubation. Samples for flow cytometry analysis were collected using the methods described above. Phytoplankton samples (15 mL) for cell counts were also collected from incubation bottles before and after the incubation period and preserved with 1% Lugol's iodine solution.

2.3. Flow cytometry analysis of prokaryotic abundance

To determine prokaryotic abundance, samples were analyzed via Beckman-Coulter CytoFLEX LX flow cytometer (Beckman-Coulter, Indianapolis, IN United States). For total prokaryotic cell abundance measurement, water samples were diluted 10 times using 1 × Tris-EDTA buffer (Sigma-Aldrich, Molecular Grade, pH 8.0). Nucleic acid stain (SYBR Green-I) was added to each sample at a final dilution of 1:10,000 and kept in darkness for 15 min at 37 °C (Marie et al., 1997). 5 μL yellowish-green fluorescent beads (Polyscience, Warrington, PA, United States) were then added to each sample as an internal standard. For autotrophic prokaryotic cell abundance measurement, samples were neither diluted nor stained. All preprepared samples were analyzed at a flow rate of 0.25 mL s^{-1} for 1 min. The software CytExpert 2.1 (Beckman-Coulter, Indianapolis, IN United States) was used to analyze the flow cytometric data. Heterotrophic prokaryote abundance was calculated by subtracting the number of autotrophic prokaryotes from total prokaryotic cell abundance in each sample.

2.4. Genomic DNA extraction, PCR, pyrosequencing and the 16S rRNA gene sequences data analysis

Genomic DNA was extracted from both the 3 μm and 0.2 μm membranes collected from all survey stations and incubation experiments (S15 and S17) following a modified enzyme/phenol-chloroform extraction protocol (Xia et al., 2020). For PCR, the V4 and V5 regions of the 16S rRNA gene were amplified using primers 515F (GTGCCAGCMGCCGCGGTAA) and 907R (CCGTCAATTCCTTTGAGTTT) (Edwardson and Hollibaugh, 2018). The PCR reaction was performed in a 30 μL reaction volume containing 15 μL of Phusion® High-Fidelity PCR Master Mix (New England Biolabs), 0.2 μM of forward and reverse primers, and about 10 ng template DNA. Thermal cycling consisted of initial denaturation at 98 °C for 30 s, followed by 25 cycles of denaturation at 98 °C for 10 s, annealing at 60 °C for 10 s and elongation at 72 °C for 10 s. Final extension was performed for 2 min at 72 °C. The amplicons were then gel-purified using the Qiagen Gel Extraction Kit (Qiagen, Germany) and sequenced on an Illumina NovaSeq platform.

The 16S rRNA gene sequences were analyzed using the microbial ecology community software Mothur, following the standard operating procedure described by Schloss et al. (2009). First, tags and primers were trimmed, and then sequences with an average quality score below 20 and lengths shorter than 300 bp were removed. Sequences were then aligned against the SILVA version 138 reference database. Chimeras were analyzed using the *chimera.uchime* command and removed. High quality sequences were identified using the SILVA database. Sequences identified as chloroplasts, mitochondria, cyanobacteria or unknown, were removed. The remaining sequences were clustered into Operational Taxonomic Units (OTUs) at cut-off values of 3%. Singletons were removed using the *remove.rare* command. Then, data were randomly subsampled at 16380 sequences per sample using the *sub.sample* command. Diversity indices (Abundance-based coverage estimator (ACE) and Shannon's diversity index (H)) were calculated using the *summary.single* command.

2.5. Metagenomic sequencing and data analysis

For metagenomic sequencing, genomic DNA was extracted from 3 μm membranes of the incubation experiment (Control and Diatom treatments only) at S17 following a modified enzyme/phenol-chloroform extraction protocol (Xia et al., 2020). Sequencing libraries were generated using NEBNext® Ultra™ DNA Library Prep Kit for Illumina (NEB, USA) following the manufacturer's recommendations. Different index codes were added to attribute sequences to each sample. The clustering of the index-coded samples was performed on a cBot Cluster Generation System according to the manufacturer's instructions (Illumina). After cluster generation, the library preparations were sequenced on an Illumina HiSeq 2500 platform and paired-end reads were generated.

Metagenomic analysis was conducted using the SqueezeMeta pipeline (Tamames and Puente-Sánchez, 2019). Metagenomic reads were quality-checked and trimmed for low-quality regions using Trimmomatic (Bolger et al., 2014). Then, sequences were assembled using Megahit with default settings (Bankevich et al., 2012). Open reading frames (ORFs) of the assembled contigs (>200 bp) were identified by the Prodigal software and were further annotated using DIAMOND against the nr, COG, KEGG, and CAZy public databases, with an e-value cutoff of 0.001 (Buchfink et al., 2015). ORFs which were affiliated with prokaryotes were retained for subsequent analysis. Raw reads were mapped to the ORFs using Bowtie to calculate the abundance of each ORF (Langmead and Salzberg, 2012). The abundance of each ORF was calculated as Transcripts Per Million (TPM): $TPM = A \times \frac{1}{\sum^{A}} \times 10^{6}$, where $A = \frac{total\ reads\ mapped\ to\ gene \times 10^{3}}{gene\ length\ in\ bp}$.

To obtain associated bacterial genomic bins, the diatom treatment metagenomic sequences were re-assembled using SPAdes with a k-mer size of 55 and 77 (Bankevich et al., 2012). The assembled contigs were clustered into potential draft genomes using MyCC (Lin and Liao, 2016), and the quality of the microbial genomes obtained were assessed using CheckM (Parks et al., 2015). One high quality genome of Planctomycetaceae (i.e., with completeness of 97.73% and contamination less than 0.01%) was further annotated using eggNOG-mapper (Huerta-Cepas et al., 2017). The metabolic pathways of the Planctomycetaceae genome were identified using KEGG Mapper (https://www.genome.jp/kegg/mapper/).

2.6. Statistical analysis

To estimate similarity among the samples, nonmetric multidimensional scaling (nMDS) analysis and hierarchical cluster analysis with an agglomeration method of "average" were conducted based on the relative abundance of OTUs in each sample using R package vegan (Dixon, 2003). Multiple regression of environmental variables with prokaryotic communities was further calculated via the *envfit* command within R package vegan. Algal densities before and after incubation were compared via Two-way ANOVA and Fisher's LSD *posthoc* analysis ($\alpha = 0.05$). Two-way ANOVA and Dunnett's *posthoc* analyzes ($\alpha = 0.05$) were performed on heterotrophic prokaryote abundances, inorganic nutrient concentrations, DOC concentrations, the ACE and Shannon's diversity index (H). Relative abundances of inoculated algae and background algae were compared before and after incubation in different treatments at each experimental station via multiple Student's t-test ($\alpha = 0.05$). Spearman analyzes ($\alpha = 0.05$) were performed via the *cor* command in R to identify the correlations among the changes of phytoplankton densities and nutrient concentrations for incubation experiments. The

abundance and diversity index of different Carbohydrate-Active Enzymes (CAZymes) modules and the abundance of different pathways in the control and diatom treatment were compared via Two-way ANOVA and Fisher's LSD *posthoc* comparisons ($\alpha = 0.05$). The Statistical Analysis of Metagenomic Profiles (STAMP) software package was used to access significant differences between prokaryotic communities (at family level) between different treatments ($\alpha = 0.05$) (Parks et al., 2014). The sequences obtained in this study have been deposited in the NCBI Sequence Read Archive (SRA) under BioProject numbers: PRJNA791015 (16S), PRJNA788358 (Metagenomes) and PRJNA789730 (genome of Planctomycetaceae Bin).

3. Results

3.1. PRE hydrographic condition and natural prokaryotic community structure

Hydrographic conditions varied with different sampling stations during the survey at PRE (Table S1). In general, surface water pH (7.75–8.50) and salinity (0.01–31.86) increased from upstream to downstream stations. Inorganic nutrient levels, including silica (0.1890–5.7678 mg Si L^{-1}), phosphate (0.0013–0.0935 mg P L^{-1}), ammonium (0.0025–0.2917 mg N L^{-1}), nitrate (0.0726–2.9099 mg N L^{-1}) and nitrite (0.0020–0.4545 mg N L^{-1}) varied with stations but generally decreased while moving from freshwater to coastal water. DOC concentrations were highly variable among stations, ranging from 1.58 to 11.17 mg L^{-1}. Heterotrophic prokaryote abundance in surface water ranged from 0.89 to 2.87 $\times$ 10^6 cells mL^{-1} according to flow cytometry analysis (Table S1).

The nMDS analysis showed a clear spatial variation of prokaryotic communities in the PRE seawater (Fig. S1). The FL prokaryotic communities were clustered into two distinct groups which were upstream (S2 to S11) and downstream clusters (S12 to S20), respectively (Fig. S1A and S1B). Inorganic nutrient levels were correlated to the upstream cluster ($p < 0.05$), and salinity and pH were correlated to the downstream cluster ($p < 0.05$) (Fig. S1A). The PA prokaryotic communities were clustered into four groups (Fig. S1C). Silica, nitrate and nitrite concentrations were strongly correlated to the cluster composed of S2, S5 and S6 ($p < 0.05$), but the rest of the clusters could not be fully explained by water quality variations (Fig. S1C and S1D).

3.2. The algal and prokaryotic growth, and nutrients change after incubation experiments

A. carterae and *T. weissflogii* had distinct responses when they were introduced to PRE. The densities of *A. carterae* remained the same before and after the incubation at S10, but decreased significantly at S17, S15 and S19 ($p < 0.01$) (Fig. 2). Meanwhile, *T. weissflogii* increased significantly at medium salinity stations (S10, $p < 0.01$; S17, $p < 0.05$), and showed no significant change at high salinity stations (S15 and S19) (Fig. 2). The cell densities of background algae were at least an order-of-magnitude lower than our algal treatments at the start of the incubation experiments (Table S2). The relative abundance of inoculated versus background algae showed contrary change pattern in all experiments except the diatom treatment at S19 (Fig. S2). This suggested that the inoculated algae and background algae could be competitors with one another. In the dinoflagellate treatments, the relative abundance of *A. carterae* only increased at S10 (Fig. S2A). At the rest of the incubation stations, *A. carterae* were out-paced by increasing background diatoms densities (Fig. S2B, S2C and S2D). In contrast, the abundances of *T. weissflogii* were high (> 95%) at all incubation stations. They significantly increased at S10 and S17 and out-paced background diatoms (Fig. S2A and S2B), but *T. weissflogii* significantly decreased at S15 where background dinoflagellates increased (Fig. S2C). The concentrations of silica, nitrate and nitrite significantly decreased after incubation in the algal treatments when compared to the control (Fig. S3B, S3C and S3D). Based on Spearman correlation analyzes, the change of silica, nitrate, ammonium and phosphate concentrations were strongly inversely correlated to the change of *T. weissflogii* cell densities ($p < 0.05$, rho < -0.7) (Fig. S4B), and the decrease of nitrite was strongly positively correlated with the increase of background diatoms in the dinoflagellate treatments ($p < 0.05$, rho < -0.7) (Fig. S4A). Thus, the decrease of inorganic nutrient concentrations is likely due to the fast-growing diatom populations. Heterotrophic prokaryote abundance increased significantly in dinoflagellate treatments at S10 ($p < 0.01$) and S15 ($p < 0.05$), and also increased significantly in diatom treatments at S17 ($p < 0.0001$), S15 ($p < 0.001$) and S19 ($p < 0.001$) (Fig. S5).

3.3. Prokaryotic community composition in diatom and dinoflagellate treatments

The ACE and Shannon's diversity index (H) for both FL and PA prokaryotes were not significantly different between the control and either algal treatment (Fig. S6). The FL prokaryotic communities did not show clear clustering in the response to the diatom and dinoflagellate treatments, except a cluster observed in diatom treatment at S17 (Fig. 3A,B). However, the PA prokaryote communities were clustered into two groups (Fig. 3C). PA prokaryotic composition was strongly influenced by the presence of diatoms, but not by the addition of dinoflagellates (Fig. 3C,D). At S15, Planctomycetaceae and Stappiaceae became more abundant in the diatom treatment ($p < 0.05$) (Fig. 4A). At S17, the relative abundance of Planctomycetaceae, Rhodobacteraceae, Stappiaceae, Cryomorphaceae and NS9_marine_group significantly increased in the diatom treatment ($p < 0.05$) (Fig. 4B). These results suggest that Planctomycetaceae and Stappiaceae in the PA prokaryotic community benefited from the diatom cells. At the OTU level, Planctomycetaceae was mainly affiliated with E_OTU2 which was identified as genus SM1A02 (Family Phycisphaeraceae) based on the SILVA database. However, we further blasted the representative sequence of E_OTU2 against the nr database and the result showed that it is highly similar with genus GMD16E07 (similarity 99.2%, NCBI accession No. AY162118) which is an unclassified Planctomycetaceae (Zengler et al., 2002) (Fig. S7). Stappiaceae was mainly composed of E_OTU12 which was identified as unclassified *Labrenzia* (Fig. S7). Dinoflagellates had relatively little impact on the PA prokaryotic community and only the Vibrionaceae significantly increased in relative abundance (S15, $p < 0.05$) (Fig. 4A).

3.4. Metagenomic sequencing statistics

To further explore the effects of the diatom treatment on the potential function of the PA prokaryotic community, a metagenomic approach was employed to analyze PA prokaryote communities in the diatom treatment and control at S17. The numbers of paired-end raw reads sequenced within each of the metagenomic samples ranged from 15.7 to 72.4 million, resulting in 674,241–1,414,602 ORFs (Table S4). Between 26.85–34.02%, 37.21–45.50% and 0.51–0.61% of the ORFs in each sequence library were annotated by the KEGG, COG and CAZy public databases, respectively (Table S4). In total, the predicted genes from assembled contigs were assigned to 492 KEGG pathways at the third level. Among these, nitrogen metabolism, CAZymes and ATP-binding cassette transporters (ABC-transporters) were investigated in detail. In general, the TPM abundances of CAZymes and ABC-transporters showed no significant difference between the diatom and control treatments, but nitrogen metabolism was significantly reduced in the diatom treatment ($p < 0.05$) (Fig. S9).

3.5. Carbohydrate metabolism of particle-attached (PA) prokaryotic communities in the diatom treatment

To compare the major carbohydrate metabolism processes between the diatom and control treatments, the predicted ORFs in each sample

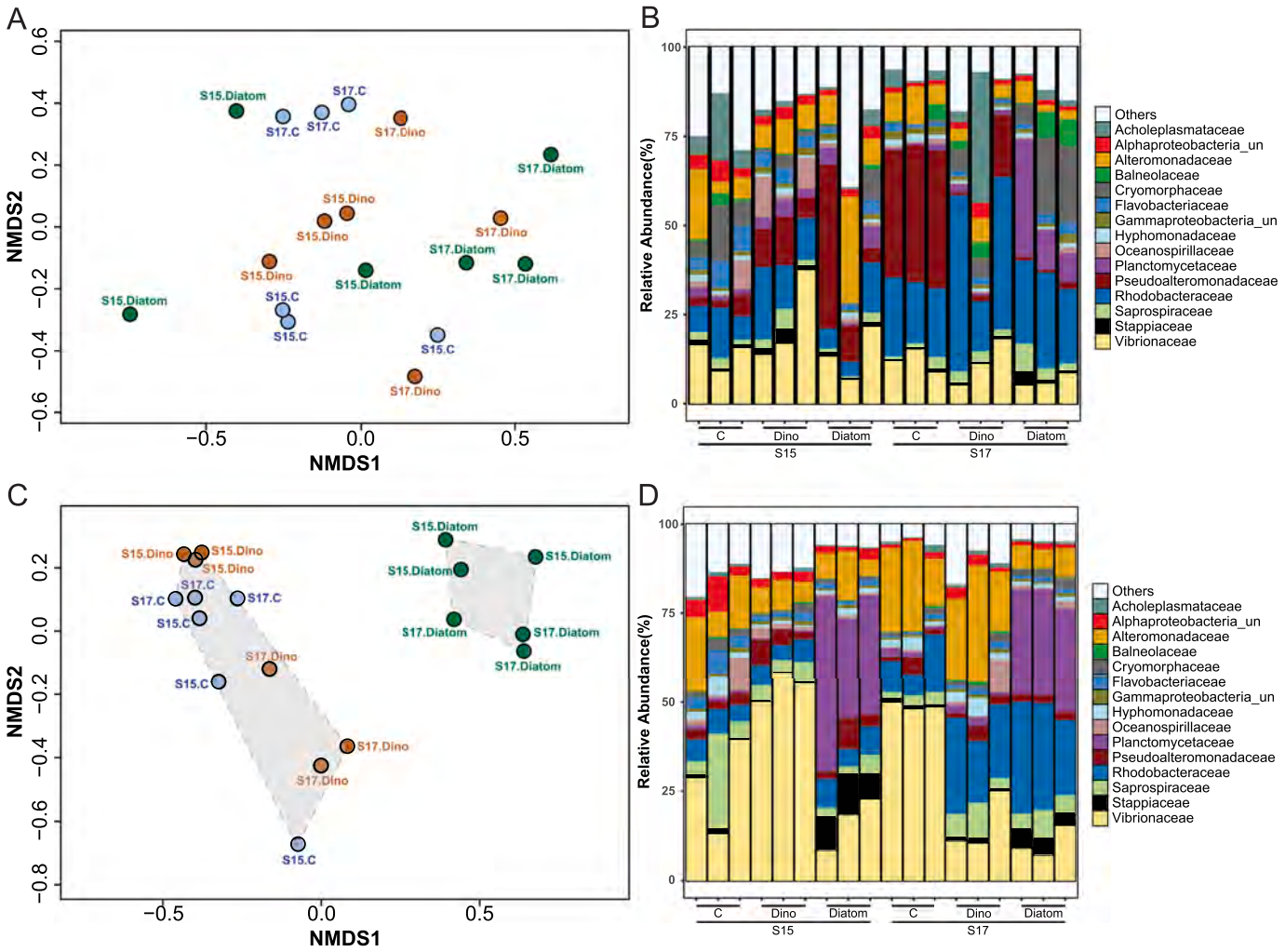

Fig. 3. nMDS analysis of (A) FL and (C) PA heterotrophic prokaryotic communities (at OTU level) after incubation in each treatment at S15 and S17 based on Bray-Curtis dissimilarity. Clusters (polygons) were determined by Hierarchical Cluster Analysis with agglomeration method of "average". The FL prokaryotic communities did not show clear clustering in response to the diatom and dinoflagellate treatments, while the PA prokaryotic composition was strongly influenced by the addition of the diatom. Community composition of (B) FL and (D) PA heterotrophic prokaryotes (at family level) after incubation in each treatment at S15 and S17.

were annotated via the CAZymes database. We observed that 110 CAZymes-related genes were significantly enhanced in the diatom treatment (Table S5). These genes belong to five CAZymes families, including Auxiliary Activities (AAs, 4 genes), Carbohydrate-Binding Modules (CBMs, 7 genes), Carbohydrate Esterases (CEs, 13 genes), Glycoside Hydrolases (GHs, 30 genes), and Glycosyl Transferases (GTs, 56 genes) (Table S5). To unveil the major carbohydrate metabolism differences of the PA prokaryotic communities between the diatom and the control treatments, the top 20 abundant CAZymes-related genes which were significantly enhanced with fold change over 2 in the diatom treatments were examined in terms of taxonomic compositions (Fig. 5 and 6A).

GHs are key enzymes that catalyze the hydrolysis of glycosidic bonds of complex carbohydrates. Five of the top 20 abundant enzyme encoding genes belong to the GHs family, which catalyze the hydrolysis of pullulan (*susA*), glycosides (*TC.GPH*), inositol (*iolG*), peptidoglycan/chitodextrins (*acm*) and maltose (*mapA*) (Fig. 5). Planctomycetes, which is mainly composed of Planctomycetaceae based on 16S rRNA results (Fig. S8), contributed to a higher relative abundance in genes of *iolG* in the diatom treatment (Student's t-test, $p < 0.05$) (Fig. 6B). Flavobacteriales_un, which is mainly composed of Cryomorphaceae based on 16S rRNA results (Fig. S8), contributed to a higher relative abundance in *susA, mapA* and *TC.GPH* in the diatom treatment (Student's t-test, $p < 0.05$) (Fig. 6B).

CEs are enzymes that catalyze the de-O- or de-N-acetylation of glycans and substituted saccharides. Three of the top 20 abundant enzyme encoding genes belong to the CEs family, which included a polyhydroxybutyrate depolymerase (*lpqC* (CE1)), an N-acetylglucosamine deacetylase (*lpxC* (CE11)) and an N-acetylglucosaminyl malate deacetylase (*bshB1* (CE14)) (Fig. 5). Planctomycetes_un (mainly composed of Planctomycetaceae, Fig. S8) contributed to higher relative abundances in genes of *lpqC* and *lpxC* in the diatom treatment relative to the control (Student's t-test, $p < 0.05$) (Fig. 6B). Rhodobacteraceae contributed higher relative abundance in genes of *lpqC* in the diatom treatment (Student's t-test, $p < 0.05$) (Fig. 6B). Flavobacteriales_un (mainly composed of Cryomorphaceae, Fig. S8) contributed to higher relative abundance in genes of *lpqC; lpxC* and *bshB1* in the diatom treatment relative to the control (Student's t-test, $p < 0.05$) (Fig. 6B).

Eleven of the top 20 abundant genes belong to the GTs family, where seven of them were classified as GT2, four as GT4 and one as GT9 (Fig. 5). Those GTs families constitute enzymes that are involved in the biosynthesis of polysaccharides. All eleven forementioned GTs encoding genes were annotated as cell membrane/envelope biogenesis in COG pathways (Table S5), suggesting that the diatom presence could promote PA prokaryotic reproduction. Regarding the taxonomic classification of these GT-related genes, Planctomycetes_un (mainly composed of Planctomycetaceae), contributed higher relative abundance in *cruC; DPM1* and *SQD2* in the diatom treatment relative to the control

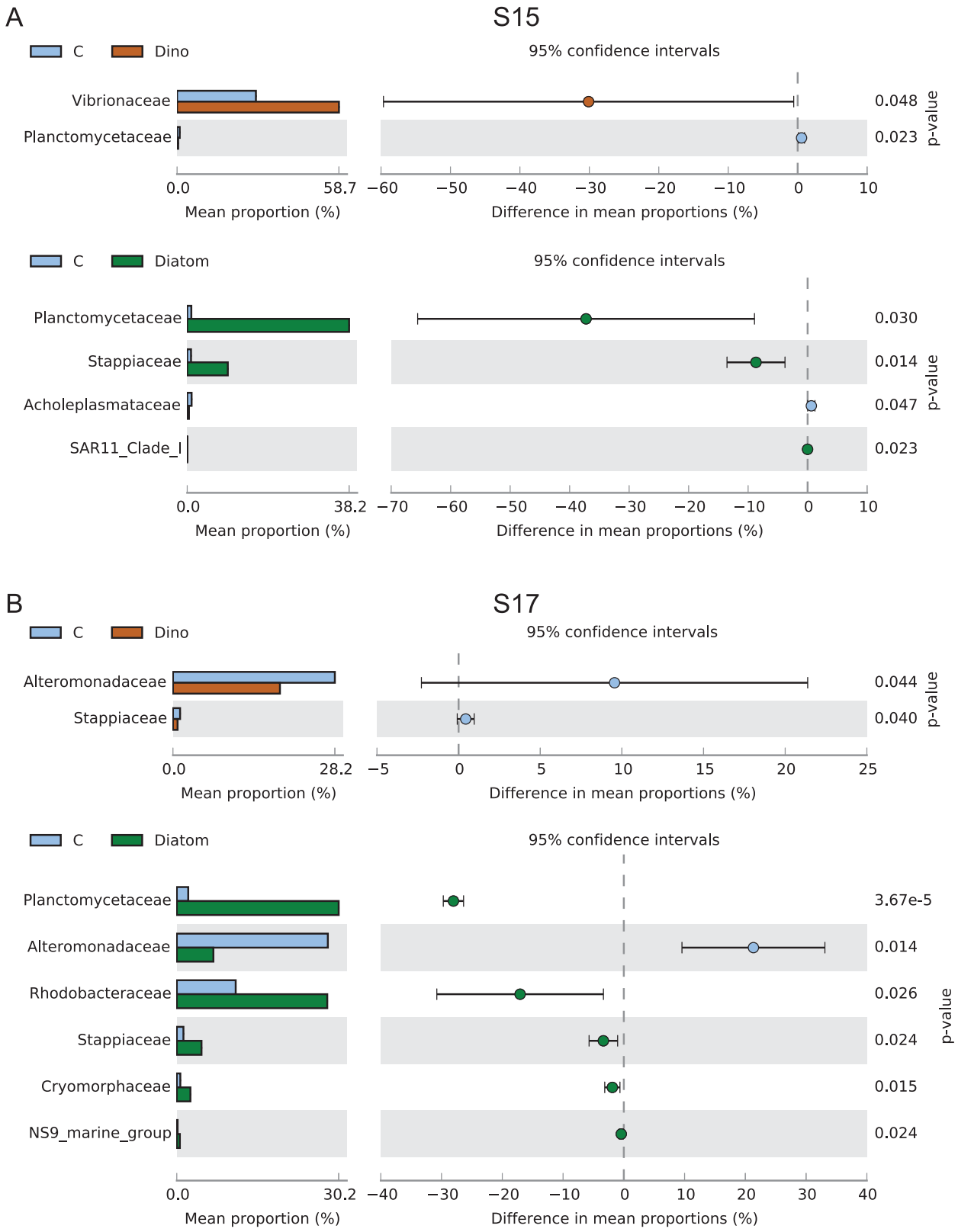

Fig. 4. STAMP analysis ($\alpha = 0.05$) of PA prokaryotic relative abundance (at family level) after incubation between different treatments at (A) S15 and (B) S17. Only significantly changed prokaryotic families were plotted ($p < 0.05$). Planctomycetaceae and Stappiaceae in the PA prokaryotic community benefited from the growth of diatom cells at both S15 and S17.

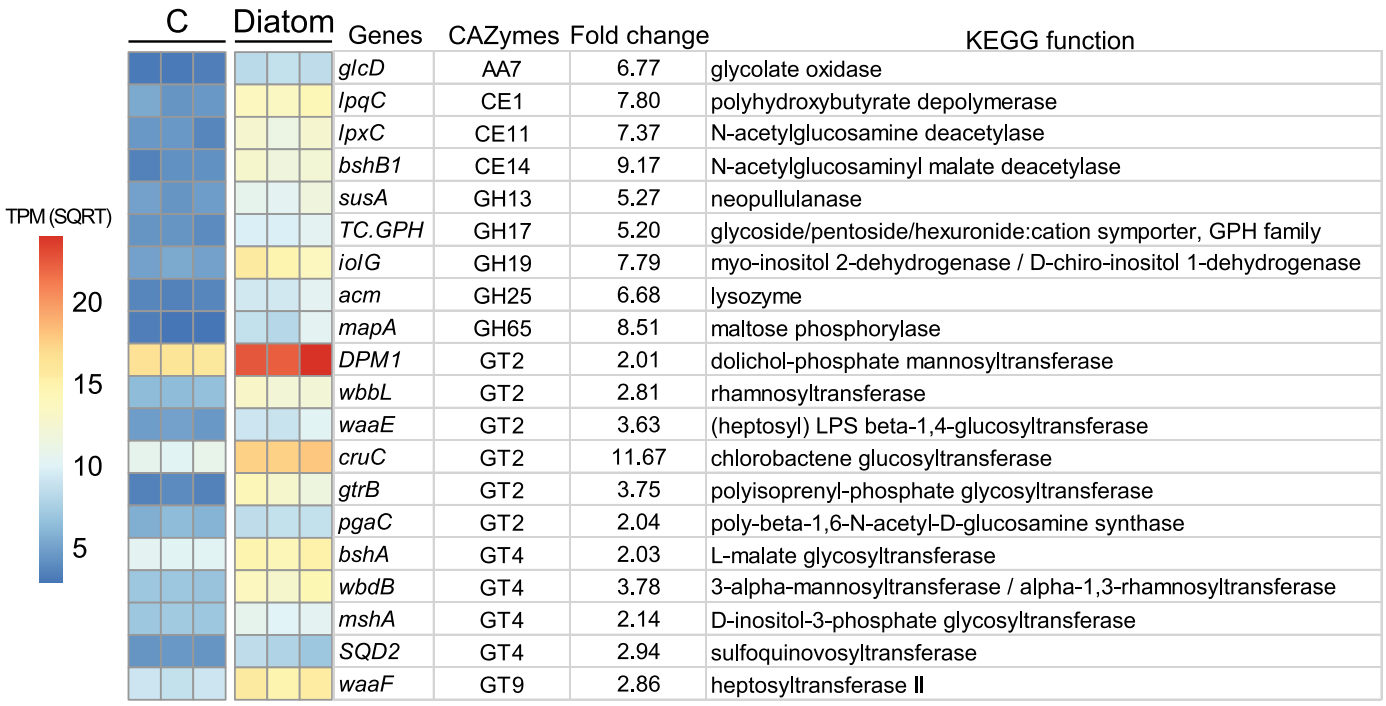

Genes	CAZymes	Fold change	KEGG function
glcD	AA7	6.77	glycolate oxidase
lpqC	CE1	7.80	polyhydroxybutyrate depolymerase
lpxC	CE11	7.37	N-acetylglucosamine deacetylase
bshB1	CE14	9.17	N-acetylglucosaminyl malate deacetylase
susA	GH13	5.27	neopullulanase
TC.GPH	GH17	5.20	glycoside/pentoside/hexuronide:cation symporter, GPH family
iolG	GH19	7.79	myo-inositol 2-dehydrogenase / D-chiro-inositol 1-dehydrogenase
acm	GH25	6.68	lysozyme
mapA	GH65	8.51	maltose phosphorylase
DPM1	GT2	2.01	dolichol-phosphate mannosyltransferase
wbbL	GT2	2.81	rhamnosyltransferase
waaE	GT2	3.63	(heptosyl) LPS beta-1,4-glucosyltransferase
cruC	GT2	11.67	chlorobactene glucosyltransferase
gtrB	GT2	3.75	polyisoprenyl-phosphate glycosyltransferase
pgaC	GT2	2.04	poly-beta-1,6-N-acetyl-D-glucosamine synthase
bshA	GT4	2.03	L-malate glycosyltransferase
wbdB	GT4	3.78	3-alpha-mannosyltransferase / alpha-1,3-rhamnosyltransferase
mshA	GT4	2.14	D-inositol-3-phosphate glycosyltransferase
SQD2	GT4	2.94	sulfoquinovosyltransferase
waaF	GT9	2.86	heptosyltransferase II

Fig. 5. Heatmap exhibiting the abundance (TPM, square root transformed) of top 20 abundant CAZymes related genes that were significantly enhanced in the diatom treatment at S17 (Student's t-test, $\alpha = 0.05$) with fold change over two, where *Fold change* $= \frac{Average\ TPM\ of\ Diatom\ treatment}{Average\ TPM\ of\ seawater\ control}$. KEGG function of each gene was also displayed in the table.

(Student's t-test, $p < 0.05$) (Fig. 6B). Rhodobacteraceae contributed higher relative abundance in *cruC* in the diatom treatment (Student's t-test, $p < 0.05$) (Fig. 6B). Flavobacteriales_un (mainly composed of Cryomorphaceae, Fig. S8), contributed higher relative abundance in genes of *bshA, DPM1, mshA, pgaC, waaF, wbbL* and *wbdB* in the diatom treatment (Student's t-test, $p < 0.05$) (Fig. 6B). Alphaproteobacteria_un, which includes Stappiaceae (Fig. S8), contributed higher relative abundance in gene of *mshA* in the diatom treatment (Student's t-test, $p < 0.05$) (Fig. 6B).

The gene *glcD*, which belongs to AAs, encodes glycolate oxidase and increased more than 6 folds in the diatom treatment relative to the control. Glycolate is one of the most abundant sources of organic carbon in the ocean, and the secretion of which by marine phytoplankton results in an estimated global annual flux of one petagram (Schada von Borzyskowski et al., 2019). Flavobacteriales_un (mainly composed of Cryomorphaceae, Fig. S8), contributed to a higher relative abundance of the *glcD* gene in the diatom treatment than the control (Student's t-test, $p < 0.05$) (Fig. 6B).

3.6. Nitrogen metabolism of particle-attached (PA) prokaryotic communities in the diatom treatment

Four nitrogen metabolism-related genes were significantly enhanced in the diatom treatment, including one glutamine synthetase encoding gene (*glnA*), two glutamate dehydrogenases encoding genes (*GLUD1_2*), and a gene encoding carbonic anhydrase (*cynT*) which is involved in the cyanate synthesis process (Fig. S10A) Planctomycetes_un (mainly composed of Planctomycetaceae, Fig. S8), contributed higher relative abundance in the *glnA* gene in the diatom treatment relative to the control (Student's t-test, $p < 0.05$) (Fig. S10B). Rhodobacteraceae contributed higher relative abundances in genes of *glnA* and *cynT* in the diatom treatment (Student's t-test, $p < 0.05$) (Fig. S10B). Flavobacteriales_un (mainly composed of Crymorphaceae, Fig. S8), contributed higher relative abundances of the genes of *glnA, GLUD1_2, cynT* and *gdhA* in the diatom treatment (Student's t-test, $p < 0.05$) (Fig. S10B). Alphaproteobacteria_un, which includes Stappiaceae (Fig. S8), contributed higher relative abundances of *cynT* gene in the diatom treatment (Student's t-test, $p < 0.05$) (Fig. S10B).

3.7. ABC-transporters for particle-attached (PA) prokaryotic communities in the diatom treatment and control

ABC-transporters constitute large varieties of membrane proteins that are responsible for the ATP-powered translocation of many substrates across membranes. Twenty-nine ABC-transporter encoding genes annotated as substrate importers were significantly enhanced in diatom treatment (Student's t-test, $p < 0.05$) (Fig. S11). Substrates included those of phospholipid (*mlaF, linL, mkl; mlaE, linK*), osmoprotectant (*opuA; opuBD*), manganese/zinc/iron (*troC, mntC, znuB; troA, mntA, znuA; troD, mntD, znuB; troB, mntB, znuC; sitD*), biotin (*bioY; bioN*), α-glucoside (*aglF, ggtC*), taurine (*tauB*), rhamnose (*rhaQ*), cellobiose (*cebF*), aspartate/glutamate/glutamine (*glnP; peb1A, glnH; gltK, aatM; gltL, aatP*) and D-allose (*alsB*).

3.8. Metabolic strategies of the abundant diatom-associated bacteria Planctomycetaceae

One high-quality genome Bin P01(i.e., completeness >97%, contamination <0.01%, evaluated using CheckM (Parks et al., 2015)), which was affiliated with the family of Planctomycetaceae was obtained from metagenomic datasets and further analyzed in detail. The abundance of this heterotrophic bacteria was greatly enhanced in the diatom treatment (Table S6, Fig. 7). The 16S rRNA gene sequence of the Planctomycetaceae Bin P01 showed 99.7% similarity with Planctomycete GMD16E07 (NCBI accession No. AY162118.1), a representative strain of Planctomycetaceae genus GMD16E07. To our knowledge, our Planctomycetaceae Bin P01 is the first genome of genus GMD16E07. The Planctomycetaceae Bin P01 genome consisted of 24 contigs with a total length of 3.91Mbp, and 3476 genes were predicted from the genome (Table S6). The GC content of the chromosomal DNA is 65.55% (Table S6). Most genes essential for chemotaxis were identified in the genome. They included the genes encoding the chemotaxis family sensor

A

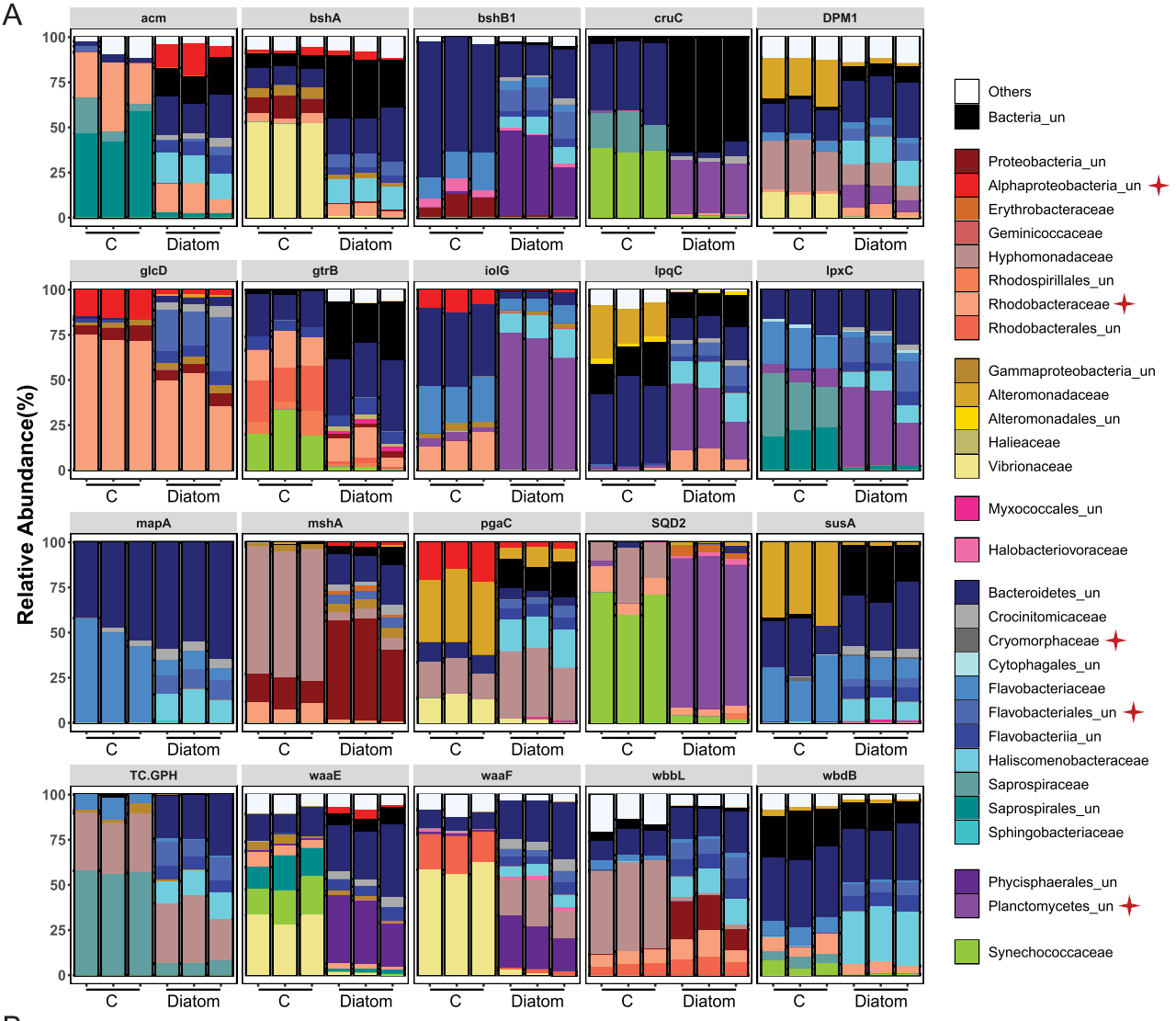

B

Genes	CAZymes	The PA prokaryotic taxa that were significantly enhanced in the diatom treatment at S17 based on 16S rRNA results			
		Planctomycetes_un (mainly composed of Planctomycetaceae)	Rhodobacteraceae	Flavobacteriales (mainly composed of Cryomorphaceae)	Alphaproteobacteria_un (includes Stappiaceae)
acm	GH25				
bshA	GT4			●	
bshB1	CE14			●	
cruC	GT3	●	●		
DPM1	GT6	●		●	
glcD	AA7			●	
gtrB	GT4				
iolG	GH19	●			
lpqC	CE1	●	●	●	
lpxC	CE11	●		●	
mapA	GH65			●	
mshA	GT4			●	●
pgaC	GT5			●	
SQD2	GT4	●			
susA	GH13			●	
TC.GPH	GH17			●	
waaE	GT7				
waaF	GT9			●	
wbbL	GT2			●	
wbdB	GT4			●	

Fig. 6. (A) Prokaryotic community composition (at family level) of top 20 abundant CAZymes related genes that were significantly enhanced in the diatom treatment at S17.✦ indicates the PA prokaryotic taxa that were significantly enhanced in the diatom treatment at S17 based on16S rRNA results. (B) A summary table of the CAZymes related genes that were significantly enhanced in the PA prokaryotic taxa highlighted by ✦ in Fig. 6A (Student's t-test, $\alpha = 0.05$).● indicates the gene that significantly increased in the corresponding taxa.

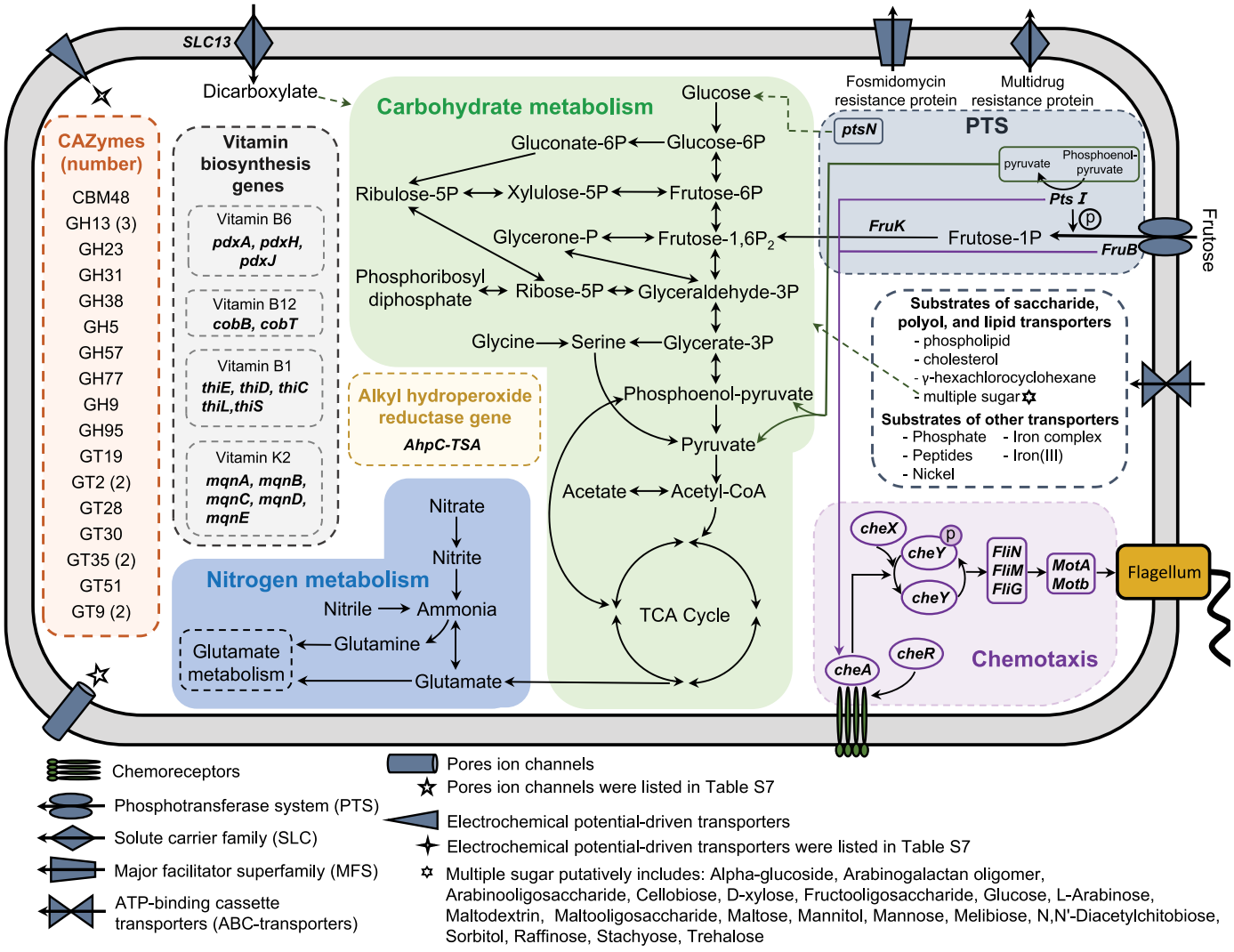

Fig. 7. Predicted metabolic pathways and properties of Planctomycetaceae Bin P01. Major carbohydrate and nitrogen metabolism pathways, CAZymes families, PTS related genes, chemotaxis related genes, vitamin biosynthesis related genes, alkyl hydroperoxide reductase gene and major transporters were plotted in the fig.. For ABC transporters, only the ones that have the genes encoding substrate-binding protein, permease protein and ATP-binding protein recovered in the genome were shown (Details in Table S7).

kinase (*cheA*), chemotaxis protein methyltransferase (*cheR*), chemotaxis proteins (*cheX, cheY, MotA* and *MotB*) and flagellar motor switch proteins (*FliG, FliN* and *FliM*) (Fig. 7), indicating their strong response to chemical stimuli.

Nine ABC-transporters were identified from the genome (only the ABC-transporters that have the genes encoding the substrate-binding protein, permease protein and ATP-binding protein recovered in the genome were calculated) (Fig. 7). Among these ABC-transporters, a multiple sugar transport was found which potentially could import nineteen different carbohydrates into the cell (Fig. 7). Also, one fructose-specific phosphotransferase system (PTS) was found in this genome. It imports and phosphorylates fructose into fructose-1-phosphate via a fructose-specific subunit (*FruB*) and a phosphoenolpyruvate-protein phosphotransferase (*ptsI*), and then further phosphorylates into fructose-1,6-bisphosphate via a 1-phosphofructokinase (*PtsK*) which eventually involves the central carbohydrate metabolism pathway, suggesting its strong ability to import and utilize fructose (Fig. 7). In addition to the fructose-specific PTS system, the gene of *ptsN* which encodes a type II enzyme in PTS system was found in the Planctomycetaceae Bin P01. This is a complex and diversified group of phosphotransferase proteins involved in controlling the intake of certain carbohydrates (e.g. glucose) and other regulatory functions (Fig. 7) (Chavarría et al., 2012). In addition, one sodium-dependent dicarboxylate transporter belonging to the solute carrier family 13 was found in the genome.

In terms of carbohydrate metabolism, the genes encoding metabolic pathways common for chemoorganotrophic bacteria, such as glycolysis, the citrate cycle and the pentose-phosphate pathway were all present in the Planctomycetaceae Bin P01 genome (Fig. 7). This strongly suggests they may be able to utilize complex carbohydrates. The genome encoded 1 CBM, 11 GHs and 10 GTs which were affiliated with 1, 9 and 7 CAZyme families, respectively (Fig. 7). The Planctomycetaceae Bin P01 was able to use both inorganic (nitrate, nitrite and ammonia) and organic (glutamine, glutamate and nitrile) sources of nitrogen (Fig. 7). Notably, one gene encoding alkyl hydroperoxide reductase, namely *AhpC-TSA,* presents in the genome. This gene is reported to reduce a wide range of reactive oxygen and nitrogen species (Alharbi et al., 2019). We also scrutinized the vitamin biosynthesis pathways. The key genes encoding vitamin B1, B6, B12 and K2 biosynthesis were found in the genome (Fig. 7).

4. Discussion

4.1. The diatom and dinoflagellate blooms showed different responses to the translocation experiment

Diatom (*Thalassiosira weissflogii*) densities increased significantly when they were exposed to ambient water conditions at different PRE stations (Fig. 2), whereas dinoflagellate (*Amphidinium carterae*) densities did not significantly increase. This may be due to diatoms generally having higher tolerances to environmental variability relative to dinoflagellates (Hill et al., 2001; Litchman, 2007). Recent "omics" studies unveiled adaptive mechanisms in the diatom *Thalassiosira pseudonana* under shifting environmental conditions, including sudden deficiencies in nitrogen and phosphorus (Chen et al., 2018; Hockin et al., 2012), silicon limitation (Mock et al., 2008), and salinity and light fluctuations (Kettles et al., 2014). Employing a range of strategies to cope with various stress factors, it is easier for this diatom to acclimate to new environments (Muhseen et al., 2015). As a group, diatoms tend to be r-strategists, quickly assimilating new nutrients and achieving high biomasses. In contrast, dinoflagellates are usually K-strategists, blooming slower than diatoms (Wasmund et al., 2017). *T. weissflogii* densities were strongly correlated with a decrease of inorganic nutrients in the incubation experiments (Spearman correlation, Fig. S4). The highest specific growth rate of *T. weissflogii* recorded in the literature is 1.24 ± 0.025 day^{-1} (Garcia et al., 2012) which is higher than that of *A. carterae* (0.93 ± 0.13 day^{-1}) (Li et al., 2016). Therefore, published growth rates for the species in this study support the idea that diatom blooms might be expected to increase more rapidly than the dinoflagellate under the right environmental conditions.

In addition to the different physiology properties between *T. weissflogii* and *A. carterae*, other conditions could also influence the re-establishment of the diatom bloom. For instance, background algae could be competitors to bloom species (Fig. S4). Besides, *in-situ* seawater conditions could also influence their response to a new environment. In the present study, we observed that *T. weissflogii* only significantly increased at S10 and S17 where the salinities were around 25 and *in-situ* concentrations of silica and nitrate were relatively high compare to S15 and S19 (Table S1). This is consistent with previous studies where *T. weissflogii* had higher growth rates at a salinity of 25 compared to rates at 30 (Garcia et al., 2012), and those growth rates had strong positive correlations with nitrate and silica concentrations (De La Rocha et al., 2010; Li et al., 2017). Moreover, a long-term phytoplankton monitoring study in the PRE showed that the proportion of diatoms have progressively increased in the PRE over the past two decades due to increasing anthropogenic nitrate inputs (Cheung et al., 2021). Considering of the demonstrated ability of diatom blooms to establish and grow, and the increasing presence of anthropogenic nutrients in the PRE, it should not be surprising if diatom blooms are increasing in frequency and intensity in this region.

4.2. The diatom bloom had strong effects on the PA prokaryotic community

In the present study, algal bloom inoculation had a significant influence on the PA prokaryotic community, but little impact on the FL prokaryotic community (Fig. 3). Other studies have found that algae and PA prokaryotes are coupled in coastal and aquatic systems (Bachmann et al., 2018; Fontanez et al., 2015; Liu et al., 2019; Rieck et al., 2015; Rösel and Grossart, 2012). We showed that the diatom bloom had stronger effects on the PA prokaryotic community compared to the dinoflagellate bloom (Fig. 3C,D). This could be due, in part, to the active growth phase of *T. weissflogii* with substantial extracellular polymeric substance (EPS) production (Gügi et al., 2015). The primary source of labile organic matter for surface ocean heterotrophic bacteria is phytoplankton (Ferrer-González et al., 2021), and maximum exportation of EPS usually occurs in the algal exponential growth phase (Staats et al., 1999). Field observations have confirmed that heterotrophic bacteria tend to follow natural algal blooms (Sperling et al., 2017; Teeling et al., 2012). Although *A. carterae* is also an EPS producer (Mandal et al., 2011), we speculate that the lack of response of PA prokaryotes in the dinoflagellate treatments may be due to the latter being in an inactive growth phase after inoculation, with minimal EPS production.

4.3. Diatom-derived carbohydrates and organic nitrogen sources shaped particle-attached (PA) prokaryotic community composition in the diatom treatment

Environment-specific responses of the PA prokaryotic community in the diatom treatment are likely due to their adaptive functionality and underlying genetic properties. The PA prokaryotes contain genes enabling a variety of metabolic capabilities, which are thought to equip cells to take advantage of patches of organic matter to grow rapidly during blooms (Luo and Moran, 2015). Therefore, the PA prokaryotic community structure is potentially influenced by substrate availability and particle quality (Bachmann et al., 2018; Yung et al., 2016). In this study, we found that the introduction of a diatom bloom shaped PA prokaryotic community composition and altered their carbon and nitrogen metabolic properties.

The significant increase of prokaryotic CAZymes-related genes results from the presence of specific carbohydrates produced and released by the diatom. Some opportunistic PA prokaryotes (e.g., Planctomycetaceae, Rhodobacteraceae and Cryomorphaceae) benefit more from these diatom-derived carbohydrates than other taxa (Figs. 5 and 6). Published studies have shown that *Thalassiosira* is able to extrude myo-inositol (Kroth et al., 2008), pullulan (Dalgic et al., 2019) and glycolate (Schada von Borzyskowski et al., 2019). In this study, the prokaryotic genes *iolG, susA* and *glcD,* which hydrolyse myo-inositol, pullulan and glycolate, respectively, were significantly increased in the diatom treatment (Fig. 5). The abundance of Planctomycetaceae significantly enhanced in the genes of *iolG*, and Cryomorphaceae presence significantly increased the genes *glcD* and *susA* (Fig. 6B). Those prokaryotes may compete against other taxa for carbohydrate use, and their increase in abundance in the diatom treatment reflects their competitive strength.

Diatom-derived carbohydrates also promote anabolic processes in opportunistic PA prokaryotes. For example, the relative abundance of Planctomycetaceae and Cryomorphaceae significantly increased in the mannosyltransferase encoding gene *DPM1* (Fig. 6), which is involved in the pathway leading to outer membrane biosynthesis (Whitfield et al., 2020), Mannose, the substrate of mannosyltransferase, has been reported as a crucial component of exudate from the diatom *T. weissflogii* (Aluwihare and Repeta, 1999). Similarly, the relative abundance Cryomorphaceae significantly increased in the Rhamnosyltransferase encoding gene *wbbL* (Fig. 6), which is involved in the synthesis of outer cell walls of gram-negative bacteria (Stevenson et al., 1994). The substrate, rhamnose is a common monosaccharide produced by *T. weissflogii* (Aluwihare and Repeta, 1999). Corresponding to the increase of *wbbL*, the gene *rhaQ,* which encodes the rhamnose import system permease protein, also significantly increased (Fig. S11). Thus, the enrichment of the both ABC-transporter genes and enzyme-encoding genes collectively provided solid evidence that rhamnose was actively transported into the prokaryotes and involved in the biosynthesis process. In general, Planctomycetaceae, Rhodobacteraceae and Cryomorphaceae all benefited from diatom-derived carbohydrates, but they appear to specialize on different components of bioreactive organic carbon.

Regarding nitrogen metabolism, one glutamine synthetase (*glnA*), two glutamate dehydrogenases (*GLUD1_2, gdhA*) and one carbonic anhydrase (*cynT*) were significantly enhanced in the diatom treatment (Fig. S10A). Organic nitrogen compounds, such as glutamine, glutamate and cyanate, are usually incorporated quickly into proteins by active prokaryotes (Newsholme et al., 2003; Palatinszky et al., 2015). Those organic nitrogen sources are likely derived from the live diatom

Thalassiosira (Bender et al., 2012). Possessing organic nitrogen metabolizing genes, the Planctomycetaceae, Rhodobacteraceae, Stappiaceae and Cryomorphaceae all benefit from diatom-derived organic nitrogen sources (Fig. S10B). We conclude that organic nitrogen secreted by diatoms attracts and fosters some opportunistic PA prokaryotes, thereby shaping the prokaryotic community. This conclusion is reinforced by the significantly elevated ABC-transporter genes that encode glutamate/glutamine-importing permease proteins (*glnP; peb1A, glnH; gltK, aatM; gltL, aatP*), implying that a substantial amount of glutamate/glutamine was assimilated by prokaryotes.

4.4. Mutualistic symbiosis between the Planctomycetaceae and *T. weissflogii* facilitated the growth and expansion of the diatom bloom

The Phycisphaeraceae (affiliated with phylum Planctomycetes) comprised up to 50% of PA prokaryotes in the diatom treatment. Genome analysis of Planctomycetaceae Bin P01 suggests that Planctomycetaceae and *T. weissflogii* have a close mutualistic association, with the diatom providing labile organic matter for the Planctomycetaceae and the bacteria supplying vitamins, detoxifying nitriles and hydrogen peroxides in exchange. A close physical connection between bacteria and algae is a prerequisite for mutualism (de-Bashan et al., 2016). The genome of Planctomycetaceae Bin P01 exhibits an intact chemotaxis pathway, considered a first step in the attachment of bacteria to algal cells and suggesting an attachment lifestyle (Sreeramana et al., 2006). In this process, the receptor kinase (*cheA*) is stimulated while the stimulatory ligands bind to chemoreceptors at the cell periphery, leading to a response at the flagellar motor (Stock et al., 1988). In addition to this well-studied chemotaxis mechanism, another receptor-independent branch of chemotactic signalling, linked to sugar uptake through PTS, was recently discovered (Neumann et al., 2012). This signal emerges from cytoplasmic PTS components (i.e.: *ptsI* and *FruB*) and transmits directly to the sensory complexes (i.e.: *CheA*) (Neumann et al., 2012). Employing a fructose-specific PTS, the Planctomycetaceae Bin P01 would be able to accurately locate a diatom cell, tracking it along fructose gradients.

Planctomycetes are thought to use phytoplankton-released polysaccharides as carbon and energy sources, probably by employing a specialized uptake and degradation system (Boedeker et al., 2017). This assumption was supported by our findings that Planctomycetaceae Bin P01 has many saccharides, polyol and lipid ABC transporters, a fructose-specific PTS and a sodium-dependent transporter for dicarboxylate. These transporters are involved in the cellular uptake of carbohydrates produced by *T. weissflogii* (Baubin et al., 2021; Gügi et al., 2015). Notably, the multiple sugar ABC-transporter can potentially uptake nineteen different carbohydrates into the cell. Many of these sugars (e.g., arabinose, glucose, mannose, rhamnose, xylose and cellulose) have been reported as major components of the secretions of the diatom *T. weissflogii* (Gügi et al., 2015). Thus, Planctomycetaceae Bin P01 is able to import different carbohydrates with high affinity to diatom-derived sugars. Carbohydrate degradation requires the production of GHs. Some specific GHs genes were identified in the Planctomycetaceae Bin P01; these are involved in the hydrolysis of the diatom-derived carbohydrates. For instance, GH38 hydrolyzes mannose (Winchester, 1984) and GH9 hydrolyzes cellobiose (Berghem and Pettersson, 1973).

Regarding nitrogen metabolism, Planctomycetaceae Bin P01 is able to utilize organic nitrogen, including nitrile, glutamine and glutamate. Notably, nitriles are a diverse group of mostly cytotoxic compounds often found in plants (Egelkamp et al., 2017). Degrading nitriles to carboxylic acids and ammonia is not only a detoxification process for both the diatom and bacteria, but also provides Planctomycetaceae itself carbon and nitrogen sources (Egelkamp et al., 2017). The metabolic properties observed here for Planctomycetaceae Bin P01 are generally consistent with a previous study where the Planctomycetaceae utilized a wide range of organic compounds (Dedysh and Ivanova, 2019), but the environmental adaptations in the present study are different and unique to the *T. weissflogii* phycosphere.

The association of the bacteria with *T. weissflogii* provides many potential benefits to the diatom. First, Planctomycetaceae could provide essential vitamins to their associated phytoplankton. The genome of Planctomycetaceae Bin P01 contains the key genes encoding the biosynthesis of vitamins B1, B6, B12 and K2, which are all important for the central metabolism of phytoplankton (Helliwell, 2017). For example, B12 plays an essential role in the metabolism of amino acids and one-carbons, while B1 is important for primary carbohydrate and amino acid metabolism (Bertrand and Allen, 2012). Additionally, the diatom is likely to benefit from the bacterial detoxification capabilities, because Planctomycetaceae Bin P01 possesses the alkyl hydroperoxide reductase gene *AhpC-TSA,* which serves as a key antioxidant enzyme and contributes to robust oxidative and nitrosative stress resistance (Alharbi et al., 2019). Hydrogen peroxide, which is predominantly produced in algal cells during photosynthesis and photorespiration, possesses a strong oxidizing potential that can damage a variety of biological molecules (Petrov and Van Breusegem, 2012). It is therefore an unwelcome by-product of normal metabolic processes in aerobic organisms (Slesak et al., 2007). Low doses of hydrogen peroxide have been successful in controlling cyanobacteria and brown tide blooms (Bauzá et al., 2014; Randhawa et al., 2012). However, a recent study has shown that heterotrophic bacteria which degrade hydrogen peroxide may protect algae against oxidative stress (Morris et al., 2011). Together, these results suggest that the close association of the Planctomycetaceae to *T. weissflogii* promotes diatom growth, and thus perpetuates the re-establishment of the bloom.

5. Conclusion

T. weissflogii and *A. carterae* populations responded differently when introduced into new environments, with the diatom population increasing more than that of the dinoflagellate. Diatom blooms may have a stronger ability to establish and grow in new locations. The introduction of an active algal blooms could be an analog for a pulse of organic matter into a new region or location, which can rapidly alter carbon and nitrogen cycling in the water column. Unlike phyto-detritus, algal blooms may produce massive amounts of bioreactive organic matter (Kamalanathan et al., 2019). The surge of these carbohydrates and organic nitrogen sources may shape PA prokaryotic community composition. Our metagenomic analyzes demonstrated that a variety of labile carbohydrates and nitrogen sources were actively transported into the cell and quickly utilized by some opportunistic PA prokaryotes, such as the Planctomycetaceae, Rhodobacteraceae and Cryomorphaceae. Further examination of the genome of Planctomycetaceae Bin P01 suggests that the Planctomycetaceae and *T. weissflogii* are likely associated in a mutualistic relationship, with the diatom providing organic matter for Planctomycetaceae and the bacteria supplying vitamins, detoxifying nitriles, and hydrogen peroxides in exchange. The proposed symbiosis facilitates the growth of the diatom and PA bacteria, thus improving the chances of successful inoculation and establishment of an algal bloom. Given the increasing frequency and severity of estuarine diatom blooms, microbial processes that respond to a growing bloom may be responsible for shaping prokaryotic communities.

Declaration of Competing Interest

The authors declare that they have no known competing financial interests or personal relationships that could have appeared to influence the work reported in this paper.

Acknowledgments

This work was supported by the CAS Pioneer Hundred Talents Program (Y8SL031001, Y9YB021001), a Key Special Project for Introduced Talents Team of Southern Marine Science and Engineering Guangdong

Laboratory (Guangzhou) (GML2019ZD0405), the National Natural Science Foundation of China (31971501, 42090042), Basic and Applied Basic Research Fund of Guangdong Province (2021A1515011522), and Institution of South China Sea Ecology and Environmental Engineering, Chinese Academy of Sciences (ISEE2021PY06). We thank Dr. Yuanyue Chen and State Key Laboratory of Tropical Oceanography, South China Sea Institute of Oceanology, Chinese Academy of Sciences for the assistance in analyzing flow cytometer samples. We also thank Dr. Yunchao Wu for analyzing nutrients and DOC samples.

Supplementary materials

Supplementary material associated with this article can be found, in the online version, at doi:10.1016/j.watres.2022.118565.

References

Alavi, M., Miller, T., Erlandson, K., Schneider, R., Belas, R., 2001. Bacterial community associated with Pfiesteria-like dinoflagellate cultures. Environ. Microbiol. 3, 380–396. https://doi.org/10.1046/j.1462-2920.2001.00207.x.

Alharbi, A., Rabadi, S.M., Alqahtani, M., Marghani, D., Worden, M., Ma, Z., Malik, M., Bakshi, C.S., 2019. Role of peroxiredoxin of the AhpC/TSA family in antioxidant defense mechanisms of Francisella tularensis. PLoS One 14, e0213699. https://doi.org/10.1371/journal.pone.0213699.

Allen, J.I., Smyth, T.J., Siddorn, J.R., Holt, M., 2008. How well can we forecast high biomass algal bloom events in a eutrophic coastal sea? Harmful Algae 8, 70–76. https://doi.org/10.1016/j.hal.2008.08.024.

Aluwihare, L., Repeta, D., 1999. A comparison of the chemical characteristics of oceanic DOM and extracellular DOM produced by marine algae. Mar. Ecol. Prog. Ser. 186, 105–117. https://doi.org/10.3354/meps186105.

Amin, S.A., Parker, M.S., Armbrust, E.V., 2012. Interactions between diatoms and bacteria. Microbiol. Mol. Biol. Rev. 76, 667–684. https://doi.org/10.1128/MMBR.00007-12.

Bachmann, J., Heimbach, T., Hassenrück, C., Kopprio, G.A., Iversen, M.H., Grossart, H. P., Gärdes, A., 2018. Environmental drivers of free-living vs. particle-attached bacterial community composition in the Mauritania upwelling system. Front. Microbiol. 9, 2836. https://doi.org/10.3389/fmicb.2018.02836.

Bankevich, A., Nurk, S., Antipov, D., Gurevich, A.A., Dvorkin, M., Kulikov, A.S., Lesin, V. M., Nikolenko, S.I., Pham, S., Prjibelski, A.D., Pyshkin, A.V., Sirotkin, A.V., Vyahhi, N., Tesler, G., Alekseyev, M.A., Pevzner, P.A., 2012. SPAdes: a new genome assembly algorithm and its applications to single-cell sequencing. J. Comput. Biol. 19, 455–477. https://doi.org/10.1089/cmb.2012.0021.

Baubin, C., Farrell, A.M., Št'ovíček, A., Ghazaryan, L., Giladi, I., Gillor, O., 2021. The role of ecosystem engineers in shaping the diversity and function of arid soil bacterial communities. Soil 7, 611–637. https://doi.org/10.5194/soil-7-611-2021.

Bauzá, L., Aguilera, A., Echenique, R., Andrinolo, D., Giannuzzi, L., 2014. Application of hydrogen peroxide to the control of Eutrophic lake systems in laboratory assays. Toxins 6, 2657–2675. https://doi.org/10.3390/toxins6092657.

Bender, S.J., Parker, M.S., Armbrust, E.V., 2012. Coupled effects of light and nitrogen source on the urea cycle and nitrogen metabolism over a diel cycle in the marine diatom *Thalassiosira pseudonana*. Protist 163, 232–251. https://doi.org/10.1016/j.protis.2011.07.008.

Berghem, L.E.R., Pettersson, L.G., 1973. The mechanism of enzymatic cellulose degradation. purification of a cellulolytic enzyme from trichoderma viride active on highly ordered cellulose. Eur. J. Biochem. 37, 21–30. https://doi.org/10.1111/j.1432-1033.1973.tb02952.x.

Berry, D.L., Goleski, J.A., Koch, F., Wall, C.C., Peterson, B.J., Anderson, O.R., Gobler, C. J., 2015. Shifts in cyanobacterial strain dominance during the onset of harmful algal blooms in Florida Bay, USA. Microb. Ecol. 70, 361–371.

Berry, M.A., Davis, T.W., Cory, R.M., Duhaime, M.B., Johengen, T.H., Kling, G.W., Marino, J.A., Den Uyl, P.A., Gossiaux, D., Dick, G.J., Denef, V.J., 2017. Cyanobacterial harmful algal blooms are a biological disturbance to Western Lake Erie bacterial communities: bacterial community ecology of CHABs. Environ. Microbiol. 19, 1149–1162. https://doi.org/10.1111/1462-2920.13640.

Bertrand, E.M., Allen, A.E., 2012. Influence of vitamin B auxotrophy on nitrogen metabolism in eukaryotic phytoplankton. Front. Microbiol. 3 https://doi.org/10.3389/fmicb.2012.00375.

Boedeker, C., Schüler, M., Reintjes, G., Jeske, O., van Teeseling, M.C.F., Jogler, M., Rast, P., Borchert, D., Devos, D.P., Kucklick, M., Schaffer, M., Kolter, R., van Niftrik, L., Engelmann, S., Amann, R., Rohde, M., Engelhardt, H., Jogler, C., 2017. Determining the bacterial cell biology of Planctomycetes. Nat. Commun. 8, 14853. https://doi.org/10.1038/ncomms14853.

Bolger, A.M., Lohse, M., Usadel, B., 2014. Trimmomatic: a flexible trimmer for illumina sequence data. Bioinformatics 30, 2114–2120. https://doi.org/10.1093/bioinformatics/btu170.

Brodie, J., Schroeder, T., Rohde, K., Faithful, J., Masters, B., Dekker, A., Brando, V., Maughan, M., 2010. Dispersal of suspended sediments and nutrients in the great barrier reef lagoon during river-discharge events: conclusions from satellite remote sensing and concurrent flood-plume sampling. Mar. Freshw. Res. 61, 651. https://doi.org/10.1071/MF08030.

Brussaard, C.P.D., Bidle, K.D., Pedrós-Alió, C., Legrand, C., 2017. The interactive microbial ocean. Nat. Microbiol. 2, 16255. https://doi.org/10.1038/nmicrobiol.2016.255.

Buchfink, B., Xie, C., Huson, D.H., 2015. Fast and sensitive protein alignment using DIAMOND. Nat. Methods 12, 59–60. https://doi.org/10.1038/nmeth.3176.

Camarena-Gómez, M.T., Ruiz-González, C., Piiparinen, J., Lipsewers, T., Sobrino, C., Logares, R., Spilling, K., 2021. Bacterioplankton dynamics driven by interannual and spatial variation in diatom and dinoflagellate spring bloom communities in the Baltic Sea. Limnol. Oceanogr. 66, 255–271. https://doi.org/10.1002/lno.11601.

Cao, X., Yu, Z., Wu, Z., Cheng, F., He, L., Yuan, Y., Song, X., Zhang, J., Zhang, Y., Zhang, W., 2017. Environmental characteristics of annual pico/nanophytoplankton blooms along the Qinhuangdao coast. Chin. J. Oceanol. Limnol. 1–12.

Chavarría, M., Kleijn, R.J., Sauer, U., Pflüger-Grau, K., de Lorenzo, V., 2012. Regulatory tasks of the phosphoenolpyruvate-phosphotransferase system of pseudomonas putida in central carbon metabolism. mBio 3. https://doi.org/10.1128/mBio.00028-12.

Chen, X.H., Li, Y.Y., Zhang, H., Liu, J.L., Xie, Z.X., Lin, L., Wang, D.Z., 2018. Quantitative proteomics reveals common and specific responses of a marine diatom *Thalassiosira pseudonana* to different macronutrient deficiencies. Front. Microbiol. 9, 2761. https://doi.org/10.3389/fmicb.2018.02761.

Cheung, Y.Y., Cheung, S., Mak, J., Liu, K., Xia, X., Zhang, X., Yung, Y., Liu, H., 2021. Distinct interaction effects of warming and anthropogenic input on diatoms and dinoflagellates in an urbanized estuarine ecosystem. Glob. Chang. Biol. 27, 3463–3473. https://doi.org/10.1111/gcb.15667.

Choi, D.H., An, S.M., Yang, E.C., Lee, H., Shim, J., Jeong, J., Noh, J.H., 2018. Daily variation in the prokaryotic community during a spring bloom in shelf waters of the East China Sea. FEMS Microbiol. Ecol. 94 https://doi.org/10.1093/femsec/fiy134.

Coyne, K.J., Wang, Y., Johnson, G., 2022. Algicidal bacteria: a review of current knowledge and applications to control harmful algal blooms. Front. Microbiol. 13, 871177 https://doi.org/10.3389/fmicb.2022.871177.

Cui, Y., Chun, S.J., Baek, S.S., Baek, S.H., Kim, P.J., Son, M., Cho, K.H., Ahn, C.Y., Oh, H. M., 2020. Unique microbial module regulates the harmful algal bloom (Cochlodinium polykrikoides) and shifts the microbial community along the Southern Coast of Korea. Sci. Total Environ. 721, 137725 https://doi.org/10.1016/j.scitotenv.2020.137725.

Dalgic, A.D., Atila, D., Karatas, A., Tezcaner, A., Keskin, D., 2019. Diatom shell incorporated PHBV/PCL-pullulan co-electrospun scaffold for bone tissue engineering. Mater. Sci. Eng. C 100, 735–746. https://doi.org/10.1016/j.msec.2019.03.046.

de-Bashan, L.E., Mayali, X., Bebout, B.M., Weber, P.K., Detweiler, A.M., Hernandez, J.P., Prufert-Bebout, L., Bashan, Y., 2016. Establishment of stable synthetic mutualism without co-evolution between microalgae and bacteria demonstrated by mutual transfer of metabolites (NanoSIMS isotopic imaging) and persistent physical association (Fluorescent in situ hybridization). Algal Res. 15, 179–186. https://doi.org/10.1016/j.algal.2016.02.019.

Dedysh, S.N., Ivanova, A.A., 2019. Planctomycetes in boreal and subarctic wetlands: diversity patterns and potential ecological functions. FEMS Microbiology Ecology 95. https://doi.org/10.1093/femsec/fiy227.

De La Rocha, C., Terbrüggen, A., Völker, C., Hohn, S., 2010. Response to and recovery from nitrogen and silicon starvation in *Thalassiosira weissflogii*: growth rates, nutrient uptake and C, Si and N content per cell. Mar. Ecol. Prog. Ser. 412, 57–68. https://doi.org/10.3354/meps08701.

Devlin, A.T., Pan, J., 2018. Dynamical Estuaries. Comprehensive Remote Sensing. Elsevier, pp. 121–144. https://doi.org/10.1016/B978-0-12-409548-9.10406-3.

Dixon, P., 2003. VEGAN, a package of R functions for community ecology. J. Veg. Sci. 14, 927–930. https://doi.org/10.1111/j.1654-1103.2003.tb02228.x.

Durham, B.P., Sharma, S., Luo, H., Smith, C.B., Amin, S.A., Bender, S.J., Dearth, S.P., Van Mooy, B.A.S., Campagna, S.R., Kujawinski, E.B., Armbrust, E.V., Moran, M.A., 2015. Cryptic carbon and sulfur cycling between surface ocean plankton. Proc. Natl. Acad. Sci. 112, 453–457. https://doi.org/10.1073/pnas.1413137112.

Edwardson, C.F., Hollibaugh, J.T., 2018. Composition and activity of microbial communities along the redox gradient of an alkaline, hypersaline, lake. Front. Microbiol. 9, 14. https://doi.org/10.3389/fmicb.2018.00014.

Egelkamp, R., Schneider, D., Hertel, R., Daniel, R., 2017. Nitrile-degrading bacteria isolated from compost. Front. Environ. Sci. 5, 56. https://doi.org/10.3389/fenvs.2017.00056.

Ferrer-González, F.X., Widner, B., Holderman, N.R., Glushka, J., Edison, A.S., Kujawinski, E.B., Moran, M.A., 2021. Resource partitioning of phytoplankton metabolites that support bacterial heterotrophy. ISME J. 15, 762–773. https://doi.org/10.1038/s41396-020-00811-y.

Fontanez, K.M., Eppley, J.M., Samo, T.J., Karl, D.M., DeLong, E.F., 2015. Microbial community structure and function on sinking particles in the north pacific subtropical gyre. Front. Microbiol. 6 https://doi.org/10.3389/fmicb.2015.00469.

Gárate-Lizárraga, I., González-Armas, R., Verdugo-Díaz, G., Okolodkov, Y.B., Pérez-Cruz, B., Díaz-Ortíz, J.A., 2019. Seasonality of the dinoflagellate *Amphidinium* cf. *carterae* (Dinophyceae: Amphidiniales) in Bahía de la Paz, Gulf of California. Mar. Pollut. Bull. 146, 532–541. https://doi.org/10.1016/j.marpolbul.2019.06.073.

Garcia, N., Lopez Elias, J.A., Miranda, A., Martinez Porchas, M., Huerta, N., Garcia, A., 2012. Effect of salinity on growth and chemical composition of the diatom *Thalassiosira weissflogii* at three culture phases. Lat. Am. J. Aquat. Res. 40, 435–440. https://doi.org/10.3856/vol40-issue2-fulltext-18.

Green, D.H., Llewellyn, L.E., Negri, A.P., Blackburn, S.I., Bolch, C.J.S., 2004. Phylogenetic and functional diversity of the cultivable bacterial community associated with the paralytic shellfish poisoning dinoflagellate Gymnodinium catenatum. FEMS Microbiol. Ecol. 47, 345–357. https://doi.org/10.1016/S0168-6496(03)00298-8.

Gügi, B., Le Costaouec, T., Burel, C., Lerouge, P., Helbert, W., Bardor, M., 2015. Diatom-specific oligosaccharide and polysaccharide structures help to unravel biosynthetic capabilities in diatoms. Mar. Drugs 13, 5993–6018. https://doi.org/10.3390/md13095993.

Helliwell, K.E., 2017. The roles of B vitamins in phytoplankton nutrition: new perspectives and prospects. New Phytol. 216, 62–68. https://doi.org/10.1111/nph.14669.

Hill, B.H., Stevenson, R.J., Pan, Y., Herlihy, A.T., Kaufmann, P.R., Johnson, C.B., 2001. Comparison of correlations between environmental characteristics and stream diatom assemblages characterized at genus and species levels. J. N. Am. Benthol. Soc. 20, 299–310. https://doi.org/10.2307/1468324.

Hockin, N.L., Mock, T., Mulholland, F., Kopriva, S., Malin, G., 2012. The response of diatom central carbon metabolism to nitrogen starvation is different from that of green algae and higher plants. Plant Physiol. 158, 299–312. https://doi.org/10.1104/pp.111.184333.

Hoff, F.H., Snell, T.W., 2007. Plankton Culture Manual, 6th edition. Florida Aqua Farms Inc.

Huerta-Cepas, J., Forslund, K., Coelho, L.P., Szklarczyk, D., Jensen, L.J., von Mering, C., Bork, P., 2017. Fast genome-wide functional annotation through orthology assignment by eggNOG-mapper. Mol. Biol. Evol. 34, 2115–2122. https://doi.org/10.1093/molbev/msx148.

Kamalanathan, M., Chiu, M.H., Bacosa, H., Schwehr, K., Tsai, S.M., Doyle, S., Yard, A., Mapes, S., Vasequez, C., Bretherton, L., Sylvan, J.B., Santschi, P., Chin, W.C., Quigg, A., 2019. Role of polysaccharides in diatom *Thalassiosira pseudonana* and its associated bacteria in hydrocarbon presence. Plant Physiol. 180, 1898–1911. https://doi.org/10.1104/pp.19.00301.

Kettles, N.L., Kopriva, S., Malin, G., 2014. Insights into the regulation of DMSP synthesis in the diatom *Thalassiosira pseudonana* through APR activity, proteomics and gene expression analyses on cells acclimating to changes in salinity, light and nitrogen. PLoS One 9, e94795. https://doi.org/10.1371/journal.pone.0094795.

Kroth, P.G., Chiovitti, A., Gruber, A., Martin-Jezequel, V., Mock, T., Parker, M.S., Stanley, M.S., Kaplan, A., Caron, L., Weber, T., Maheswari, U., Armbrust, E.V., Bowler, C., 2008. A model for carbohydrate metabolism in the diatom phaeodactylum tricornutum deduced from comparative whole genome analysis. PLoS One 3, e1426. https://doi.org/10.1371/journal.pone.0001426.

Langmead, B., Salzberg, S.L., 2012. Fast gapped-read alignment with Bowtie 2. Nat. Methods 9, 357–359. https://doi.org/10.1038/nmeth.1923.

Li, L., Lü, S., Cen, J., 2019. Spatio-temporal variations of harmful algal blooms along the coast of Guangdong, Southern China during 1980–2016. J. Oceanol. Limnol. 37, 535–551.

Li, M., Shi, X., Guo, C., Lin, S., 2016. Phosphorus deficiency inhibits cell division but not growth in the dinoflagellate *Amphidinium carterae*. Front. Microbiol. 7 https://doi.org/10.3389/fmicb.2016.00826.

Li, W., Yang, Y., Li, Z., Xu, J., Gao, K., 2017. Effects of seawater acidification on the growth rates of the diatom *Thalassiosira* (Conticribra) *weissflogii* under different nutrient, light, and UV radiation regimes. J. Appl. Phycol. 29, 133–142. https://doi.org/10.1007/s10811-016-0944-y.

Li, Y., Zhao, Q., Lü, S., 2013. The genus Thalassiosira off the Guangdong coast, South China Sea. Bot. Mar. 56 https://doi.org/10.1515/bot-2011-0045.

Lin, H.H., Liao, Y.C., 2016. Accurate binning of metagenomic contigs via automated clustering sequences using information of genomic signatures and marker genes. Sci. Rep. 6, 24175. https://doi.org/10.1038/srep24175.

Litchman, E., 2007. Resource competition and the ecological success of phytoplankton. Evolution of Primary Producers in the Sea. Elsevier, pp. 351–375. https://doi.org/10.1016/B978-012370518-1/50017-5.

Liu, M., Liu, L., Chen, H., Yu, Z., Yang, J.R., Xue, Y., Huang, B., Yang, J., 2019. Community dynamics of free-living and particle-attached bacteria following a reservoir microcystis bloom. Sci. Total Environ. 660, 501–511. https://doi.org/10.1016/j.scitotenv.2018.12.414.

Lu, D., Qi, Y., Gu, H., Dai, X., Wang, H., Gao, Y., Shen, P.P., Zhang, Q., Yu, R., Lu, S., 2014. Causative species of harmful algal blooms in Chinese coastal waters. Algol. Stud. 145–146, 145–168. https://doi.org/10.1127/1864-1318/2014/0161.

Luo, H., Moran, M.A., 2015. How do divergent ecological strategies emerge among marine bacterioplankton lineages? Trends Microbiol. 23, 577–584. https://doi.org/10.1016/j.tim.2015.05.004.

Mandal, S.K., Singh, R.P., Patel, V., 2011. Isolation and characterization of exopolysaccharide secreted by a toxic dinoflagellate, *Amphidinium carterae* hulburt 1957 and its probable role in harmful algal blooms (HABs). Microb. Ecol. 62, 518–527. https://doi.org/10.1007/s00248-011-9852-5.

Marie, D., Partensky, F., Jacquet, S., Vaulot, D., 1997. Enumeration and cell cycle analysis of natural populations of marine picoplankton by flow cytometry using the nucleic acid stain SYBR green I. Appl. Environ. Microbiol. 63, 186–193. https://doi.org/10.1128/aem.63.1.186-193.1997.

Mock, T., Samanta, M.P., Iverson, V., Berthiaume, C., Robison, M., Holtermann, K., Durkin, C., BonDurant, S.S., Richmond, K., Rodesch, M., Kallas, T., Huttlin, E.L., Cerrina, F., Sussman, M.R., Armbrust, E.V., 2008. Whole-genome expression profiling of the marine diatom *Thalassiosira pseudonana* identifies genes involved in silicon bioprocesses. Proc. Natl. Acad. Sci. 105, 1579–1584. https://doi.org/10.1073/pnas.0707946105.

Morris, J.J., Johnson, Z.I., Szul, M.J., Keller, M., Zinser, E.R., 2011. Dependence of the cyanobacterium prochlorococcus on hydrogen peroxide scavenging microbes for growth at the ocean's surface. PLoS One 6, e16805. https://doi.org/10.1371/journal.pone.0016805.

Muhseen, Z.T., Xiong, Q., Chen, Z., Ge, F., 2015. Proteomics studies on stress responses in diatoms. Proteomics 15, 3943–3953. https://doi.org/10.1002/pmic.201500165.

Neumann, S., Grosse, K., Sourjik, V., 2012. Chemotactic signaling via carbohydrate phosphotransferase systems in *Escherichia coli*. Proc. Natl. Acad. Sci. 109, 12159–12164. https://doi.org/10.1073/pnas.1205307109.

Newsholme, P., Lima, M.M.R., Procopio, J., Pithon-Curi, T.C., Doi, S.Q., Bazotte, R.B., Curi, R., 2003. Glutamine and glutamate as vital metabolites. Braz. J. Med. Biol. Res. 36, 153–163. https://doi.org/10.1590/S0100-879X2003000200002.

Paerl, H.W., Otten, T.G., Kudela, R., 2018. Mitigating the expansion of harmful algal blooms across the freshwater-to-marine continuum. Environ. Sci. Technol. 52, 5519–5529. https://doi.org/10.1021/acs.est.7b05950.

Palatinszky, M., Herbold, C., Jehmlich, N., Pogoda, M., Han, P., von Bergen, M., Lagkouvardos, I., Karst, S.M., Galushko, A., Koch, H., Berry, D., Daims, H., Wagner, M., 2015. Cyanate as an energy source for nitrifiers. Nature 524, 105–108. https://doi.org/10.1038/nature14856.

Pan, J., Lai, W., Thomas Devlin, A., Pan, J., Devlin, A., 2020. Circulations in the pearl river estuary: observation and modeling. Estuaries and Coastal Zones - Dynamics and Response to Environmental Changes. IntechOpen. https://doi.org/10.5772/intechopen.91058.

Parks, D.H., Imelfort, M., Skennerton, C.T., Hugenholtz, P., Tyson, G.W., 2015. CheckM: assessing the quality of microbial genomes recovered from isolates, single cells, and metagenomes. Genome Res. 25, 1043–1055. https://doi.org/10.1101/gr.186072.114.

Parks, D.H., Tyson, G.W., Hugenholtz, P., Beiko, R.G., 2014. STAMP: statistical analysis of taxonomic and functional profiles. Bioinformatics 30, 3123–3124. https://doi.org/10.1093/bioinformatics/btu494.

Petrov, V.D., Van Breusegem, F., 2012. Hydrogen peroxide—a central hub for information flow in plant cells. AoB Plants 2012. https://doi.org/10.1093/aobpla/pls014.

Phlips, E.J., Badylak, S., Lasi, M.A., Chamberlain, R., Green, W.C., Hall, L.M., Hart, J.A., Lockwood, J.C., Miller, J.D., Morris, L.J., Steward, J.S., 2015. From red tides to green and brown tides: bloom dynamics in a restricted subtropical lagoon under shifting climatic conditions. Estuaries Coasts 38, 886–904.

Ramanan, R., Kim, B.H., Cho, D.H., Oh, H.M., Kim, H.S., 2016. Algae–bacteria interactions: evolution, ecology and emerging applications. Biotechnol. Adv. 34, 14–29. https://doi.org/10.1016/j.biotechadv.2015.12.003.

Randhawa, V., Thakkar, M., Wei, L., 2012. Applicability of hydrogen peroxide in brown tide control – culture and microcosm studies. PLoS One 7, e47844. https://doi.org/10.1371/journal.pone.0047844.

Rieck, A., Herlemann, D.P.R., Jürgens, K., Grossart, H.P., 2015. Particle-associated differ from free-living bacteria in surface waters of the Baltic sea. Front. Microbiol. 6 https://doi.org/10.3389/fmicb.2015.01297.

Rösel, S., Grossart, H., 2012. Contrasting dynamics in activity and community composition of free-living and particle-associated bacteria in spring. Aquat. Microb. Ecol. 66, 169–181. https://doi.org/10.3354/ame01568.

Schada von Borzyskowski, L., Severi, F., Krüger, K., Hermann, L., Gilardet, A., Sippel, F., Pommerenke, B., Claus, P., Cortina, N.S., Glatter, T., Zauner, S., Zarzycki, J., Fuchs, B.M., Bremer, E., Maier, U.G., Amann, R.I., Erb, T.J., 2019. Marine proteobacteria metabolize glycolate via the β-hydroxyaspartate cycle. Nature 575, 500–504. https://doi.org/10.1038/s41586-019-1748-4.

Schloss, P.D., Westcott, S.L., Ryabin, T., Hall, J.R., Hartmann, M., Hollister, E.B., Lesniewski, R.A., Oakley, B.B., Parks, D.H., Robinson, C.J., Sahl, J.W., Stres, B., Thallinger, G.G., Van Horn, D.J., Weber, C.F., 2009. Introducing mothur: open-source, platform-independent, community-supported software for describing and comparing microbial communities. Appl. Environ. Microbiol. 75, 7537–7541. https://doi.org/10.1128/AEM.01541-09.

Schmidt, M.L., White, J.D., Denef, V.J., 2016. Phylogenetic conservation of freshwater lake habitat preference varies between abundant bacterioplankton phyla: Bacterial habitat preferences in freshwater lakes. Environ. Microbiol. 18, 1212–1226. https://doi.org/10.1111/1462-2920.13143.

Seebah, S., Fairfield, C., Ullrich, M.S., Passow, U., 2014. Aggregation and sedimentation of *Thalassiosira weissflogii* (diatom) in a warmer and more acidified future ocean. PLoS One 9, e112379. https://doi.org/10.1371/journal.pone.0112379.

Slesak, I., Libik, M., Karpinska, B., Karpinski, S., Miszalski, Z., 2007. The role of hydrogen peroxide in regulation of plant metabolism and cellular signalling in response to environmental stresses. Acta Biochim. Pol. 54, 39–50. https://doi.org/10.18388/abp.2007_3267.

Sperling, M., Piontek, J., Engel, A., Wiltshire, K.H., Niggemann, J., Gerdts, G., Wichels, A., 2017. Combined Carbohydrates Support Rich Communities of Particle-Associated Marine Bacterioplankton. Front. Microbiol. 08 https://doi.org/10.3389/fmicb.2017.00065.

Sreeramana, S., M, M., R, N.M., S, M., X, R., 2006. Chemotaxis movement and attachment of agrobacterium tumefaciens to banana tissues. Biotechnology 5, 198–202. https://doi.org/10.3923/biotech.2006.198.202 (Faisalabad).

Staats, N., De Winder, B., Stal, L., Mur, L., 1999. Isolation and characterization of extracellular polysaccharides from the epipelic diatoms *Cylindrotheca closterium* and *Navicula salinarum*. Eur. J. Phycol. 34, 161–169. https://doi.org/10.1080/09670269910001736212.

Stevenson, G., Neal, B., Liu, D., Hobbs, M., Packer, N.H., Batley, M., Redmond, J.W., Lindquist, L., Reeves, P., 1994. Structure of the O antigen of Escherichia coli K-12 and the sequence of its rfb gene cluster. J. Bacteriol. 176, 4144–4156. https://doi.org/10.1128/JB.176.13.4144-4156.1994.

Stock, A., Chen, T., Welsh, D., Stock, J., 1988. CheA protein, a central regulator of bacterial chemotaxis, belongs to a family of proteins that control gene expression in response to changing environmental conditions. Proc. Natl. Acad. Sci. 85, 1403–1407. https://doi.org/10.1073/pnas.85.5.1403.

Stumpf, R.P., Tomlinson, M.C., Calkins, J.A., Kirkpatrick, B., Fisher, K., Nierenberg, K., Currier, R., Wynne, T.T., 2009. Skill assessment for an operational algal bloom

forecast system. J. Mar. Syst. 76, 151–161. https://doi.org/10.1016/j.jmarsys.2008.05.016.

Sun, R., Sun, P., Zhang, J., Esquivel-Elizondo, S., Wu, Y., 2018. Microorganisms-based methods for harmful algal blooms control: a review. Bioresour. Technol. 248, 12–20. https://doi.org/10.1016/j.biortech.2017.07.175.

Tamames, J., Puente-Sánchez, F., 2019. SqueezeMeta, a highly portable, fully automatic metagenomic analysis pipeline. Front. Microbiol. 9, 3349. https://doi.org/10.3389/fmicb.2018.03349.

Teeling, H., Fuchs, B.M., Becher, D., Klockow, C., Gardebrecht, A., Bennke, C.M., Kassabgy, M., Huang, S., Mann, A.J., Waldmann, J., Weber, M., Klindworth, A., Otto, A., Lange, J., Bernhardt, J., Reinsch, C., Hecker, M., Peplies, J., Bockelmann, F. D., Callies, U., Gerdts, G., Wichels, A., Wiltshire, K.H., Glockner, F.O., Schweder, T., Amann, R., 2012. Substrate-controlled succession of marine bacterioplankton populations induced by a phytoplankton bloom. Science 336, 608–611. https://doi.org/10.1126/science.1218344.

Tester, P.A., Stumpf, R.P., Vukovich, F.M., Fowler, P.K., Turner, J.T., 1991. An expatriate red tide bloom: transport, distribution, and persistence. Limnol. Oceanogr. 36, 1053–1061. https://doi.org/10.4319/lo.1991.36.5.1053.

Wasmund, N., Kownacka, J., Göbel, J., Jaanus, A., Johansen, M., Jurgensone, I., Lehtinen, S., Powilleit, M., 2017. The diatom/dinoflagellate index as an indicator of ecosystem changes in the Baltic Sea 1. Principle and handling instruction. Front. Mar. Sci. 4 https://doi.org/10.3389/fmars.2017.00022.

Wemheuer, B., Güllert, S., Billerbeck, S., Giebel, H.A., Voget, S., Simon, M., Daniel, R., 2014. Impact of a phytoplankton bloom on the diversity of the active bacterial community in the southern North Sea as revealed by metatranscriptomic approaches. FEMS Microbiol. Ecol. 87, 378–389. https://doi.org/10.1111/1574-6941.12230.

Whitfield, C., Williams, D.M., Kelly, S.D., 2020. Lipopolysaccharide O-antigens—bacterial glycans made to measure. J. Biol. Chem. 295, 10593–10609. https://doi.org/10.1074/jbc.REV120.009402.

Winchester, B., 1984. Role of α-d-mannosidases in the biosynthesis and catabolism of glycoproteins. Biochem. Soc. Trans. 12, 522–524. https://doi.org/10.1042/bst0120522.

Xia, X., Ki Leung, S., Cheung, S., Zhang, S., Liu, H., 2020. Rare bacteria in seawater are dominant in the bacterial assemblage associated with the bloom-forming dinoflagellate Noctiluca scintillans. Sci. Total Environ. 711, 135107 https://doi.org/10.1016/j.scitotenv.2019.135107.

Yong, J.J.J.Y., Chew, K.W., Khoo, K.S., Show, P.L., Chang, J.S., 2021. Prospects and development of algal-bacterial biotechnology in environmental management and protection. Biotechnol. Adv. 47, 107684 https://doi.org/10.1016/j.biotechadv.2020.107684.

Yung, C.M., Ward, C.S., Davis, K.M., Johnson, Z.I., Hunt, D.E., 2016. Insensitivity of diverse and temporally variable particle-associated microbial communities to bulk seawater environmental parameters. Appl. Environ. Microbiol. 82, 3431–3437. https://doi.org/10.1128/AEM.00395-16.

Zengler, K., Toledo, G., Rappe, M., Elkins, J., Mathur, E.J., Short, J.M., Keller, M., 2002. Nonlinear partial differential equations and applications: cultivating the uncultured. Proc. Natl. Acad. Sci. 99, 15681–15686. https://doi.org/10.1073/pnas.252630999.

Zhang, H., Wang, K., Shen, L., Chen, H., Hou, F., Zhou, X., Zhang, D., Zhu, X., 2018. Microbial community dynamics and assembly follow trajectories of an early-spring diatom bloom in a semienclosed bay. Appl. Environ. Microbiol. 84 https://doi.org/10.1128/AEM.01000-18.

Zhou, J., Lao, Y., Song, J., Jin, H., Zhu, J., Cai, Z., 2020. Temporal heterogeneity of microbial communities and metabolic activities during a natural algal bloom. Water Res. 183, 116020 https://doi.org/10.1016/j.watres.2020.116020.

Zhou, J., Richlen, M.L., Sehein, T.R., Kulis, D.M., Anderson, D.M., Cai, Z., 2018. Microbial community structure and associations during a marine dinoflagellate bloom. Front. Microbiol. 9 https://doi.org/10.3389/fmicb.2018.01201.